Convergence Properties of a Class of Boundary Element Approximations to Linear Diffusion Problems with Localized Nonlinear Reactions

Anthony P. Peirce, Attila Askar, and Herschel Rabitz
Department of Mathematics and Statistics, McMaster University, Hamilton, Ontario L8S 4K1, Canada; Mathematics Department, Bogazici University, Bebek-Istanbul, Turkey; and Department of Chemistry, Princeton University, Princeton, NJ 08544

We consider a boundary element (BE) Algorithm for solving linear diffusion desorption problems with localized nonlinear reactions. The proposed BE algorithm provides an elegant representation of the effect of localized nonlinear reactions, which enables the effects of arbitrarily oriented defect structures to be incorporated into BE models without having to perform severe mesh deformations.

We propose a one-step recursion procedure to advance the BE solution of linear diffusion localized nonlinear reaction problems and investigate its convergence properties. The separation of the linear and nonlinear effects by the boundary integral formulation enables us to consider the convergence properties of approximations to the linear terms and nonlinear terms of the boundary integral equation separately.

For the linear terms we investigate how the degree of piecewise polynomial collocation in space and the size of the spatial mesh relative to the time step affects the accumulation of errors in the one-step recursion scheme. We develop a novel convergence analysis that combines asymptotic methods with Lax's Equivalence Theorem. We identify a dimensionless meshing parameter Θ whose magnitude governs the performance of the one-step BE schemes. In particular, we show that piecewise constant (PWC) and piecewise linear (PWL) BE schemes are conditionally convergent, have lower asymptotic bounds placed on the size of time steps, and which display excess numerical diffusion when small time steps are used. There is no asymptotic bound on how large the tie steps can be—this allows the solution to be advanced in fewer, larger time steps. The piecewise quadratic (PWQ) BE scheme is shown to be unconditionally convergent; there is no asymptotic restriction on the relative sizes of the time and spatial meshing and no numerical diffusion. We verify the theoretical convergence properties in numerical examples. This analysis provides useful information about the appropriate degree of spatial piecewise polynomial and the meshing strategy for a given problem.

For the nonlinear terms we investigate the convergence of an explicit algorithm to advance the solution at an active site forward in time by means of Caratheodory iteration combined with piecewise linear interpolation. We consider a model problem comprising a singular nonlinear Volterra equation that represents the effect of the term in the BE formulation that is due to a single defect. We prove the convergence of the piecewise linear Caratheodory iteration algorithm to a solution of the model problem for as long as such a solution can be shown to exist. This analysis provides a theoretical justification for the use of piecewise linear Caratheodory iterates for advancing the effects of localized reactions.

Numerical Methods for Partial Differential Equations, 6, 75–108 (1990)
© 1990 John Wiley & Sons, Inc. CCC 0749-159X/90/01075-34$04.00

I. INTRODUCTION

A problem of significant physical interest is the linear diffusion equation with localized nonlinear reactions representing, for example, the influence of defects on a catalytic surface [1–3]. We advocate the use of a boundary element (BE) algorithm [4–7] for solving these linear diffusion-desorption problems with localized nonlinear defect reactions. The proposed BE algorithm provides an elegant representation of localized nonlinear reactions in which the effect of defect reactions is incorporated by adding a term to the standard BE formulation for heat conduction. This separation of linear and nonlinear terms in the integral equation enables the effects of arbitrarily oriented defect structures to be incorporated into the model without having to disturb the mesh used to propagate the linear part of the solution. More traditional methods for solving diffusion problems such as finite difference and finite element methods provide poor representations of localized reactions and would require severe mesh deformation to incorporate the effects of arbitrarily oriented defect structures.

We desire the solution of the diffusion localized reaction problem throughout the spatial domain of the problem for each time-step. Because of this requirement we choose to advance the BE solution by means of a one-step recursion process in which the solution throughout the spatial domain is carried from one time level to the next and then used as initial data for the following time step. A second time marching strategy, commonly used in the BE solution of linear diffusion problems, is to calculate boundary data for all time and solution values at selected interior points within the spatial domain. The one-step recursion procedure is very similar to explicit time marching schemes for finite difference and finite element spatial discretizations of the diffusion equation. The main difference in the case of the one-step BE discretization is that the matrix communicating the solution from one time level to the next is fully populated whereas the corresponding matrices for the finite difference and finite element methods are sparse. This is apparently a distinct computational disadvantage of the one-step BE procedure. However, the Fast Fourier Transform can be used to exploit the convolution form of the discretized BE equations to yield a more efficient and competitive algorithm. Our ultimate objective is to use the accurate representation of localized reactions as provided by the BE algorithm, and not to search for a more efficient algorithm for solving the linear diffusion equation. Therefore, we restrict our investigation to the convergence properties of the one-step BE procedure for solving linear diffusion localized reaction problems. Consistent with this objective, we will restrict comparisons between the BE algorithm and finite difference and finite element methods to discussion of the qualitative differences between these algorithms.

The separation of the linear and nonlinear effects by the boundary integral formulation will form the basis for our investigation of the convergence properties of the one-step BE procedure.

Analysis of Linear Effects

The one-step recursion procedure relies heavily on the spatial discretization of the linear part of the integral equation to communicate the effects of preced-

ing time steps to subsequent time steps. We investigate the manner in which the degree of piecewise polynomial collocation in space and the size of the spatial mesh relative to the time step affects the accumulation of errors in the one-step recursion scheme. We develop a novel convergence analysis that combines asymptotic methods with Lax's Equivalence Theorem [8]. It is possible to identify a dimensionless meshing parameter Θ whose magnitude governs the performance of the one-step BE schemes. Although the one-step BE schemes have a similar form to explicit finite difference and finite element schemes, their space-time mesh requirements are very different.

We verify the convergence properties predicted by the asymptotic analysis in numerical examples. The close correspondence between the theoretical predictions and the numerical results validates the assumption that the major error accumulation is due to the spatial discretization. The insight gained from the analysis presented in this paper should prove useful in the choice of the appropriate degree of piecewise polynomial to use in the spatial discretization and the meshing strategy for a given problem. Although the analysis performed here is restricted to one-dimensional problems, it can, in principle, be extended to higher dimensions. Numerical evidence suggests that the same phenomena of numerical diffusion persists in two dimensions for schemes based on piecewise constant and piecewise linear interpolation.

Analysis of Nonlinear Effects

We propose an explicit algorithm to advance the solution at an active site forward in time. The algorithm combines Caratheodory iteration with piecewise linear interpolation to form an explicit time marching scheme. Since the BE formulation separates the linear and nonlinear effects we assume that the time-advancement of the linear effects is convergent according to the linear analysis discussed above. Therefore, our analysis concentrates on the performance of the piecewise linear Caratheodory iteration algorithm when it is used to advance the solution at a single active site at which a nonlinear reaction process is assumed to occur. We consider a model problem that includes the term in the BE formulation that is due to a single defect. Alternatively, the model problem may be viewed as a singular nonlinear Volterra equation to which the BE formulation reduces for certain special geometries. We prove the convergence of the piecewise linear Caratheodory iteration algorithm to a solution of the model problem for as long as such a solution can be shown to exist. This analysis provides a theoretical justification for the use of piecewise linear Caratheodory iteration for advancing the effects of localized reactions in linear diffusion localized nonlinear reaction problems.

Analyses of numerical methods based on the boundary integral formulation of the linear diffusion equation have been considered [9, 10]. These analyses are more appropriate for the second time-marching strategy described above, the primary goal of which is to determine the boundary unknowns and from these the solution values at only selected interior points within the spatial domain. These analyses assume that the solution vanishes when $t = 0$ and therefore will give no account of the error due to the approximation of the spatial convolution

integral of the Green's function and the initial condition, which dominates the error in the one-step recursion algorithm studied in this paper. Moreover, if the initial conditions were not zero, the second time-marching strategy would require the evaluation of the spatial convolution integral for times that are typically large. In this case, the effect of errors in approximating this integral will be subdominant to errors in approximating the boundary integrals. Therefore, the linear convergence analysis of the one-step iteration procedure presented in this paper is quite distinct from the previous analyses mentioned. As can be expected the phenomenon of numerical diffusion, which is explored in this paper, was not predicted by previous analyses as they did not discuss any of the essential features of the one-step recursion procedure.

In Section 2 the governing linear diffusion localized nonlinear reaction equations are introduced and the representation of this problem as a boundary integral equation is presented. In Section 3 we analyze the convergence properties of the one-step recursion algorithm when used to advance the BE approximations to the linear diffusion equation. Stability of the discretized BE equations is established using discrete Fourier transforms. Consistency is investigated using asymptotic methods. The theoretical and practical implications of the convergence analysis are discussed. A numerical verification of the convergence properties is provided. In Section 4 we discuss the convergence of an explicit algorithm to advance the solution at localized reaction sites. By assuming certain special geometries, the problem is reduced to a model problem involving a singular nonlinear Volterra equation. A piecewise linear Caratheodory iteration scheme is proposed for the Volterra equation. The existence theory of Miller [11] is used to establish convergence of the piecewise linear Caratheodory iterates to a solution of the Volterra equation for as long as such a solution is guaranteed to exist by the Miller theory. The piecewise linear collocation scheme is applied to two simple problems. In one, the localized reactions are linear and the approximate and analytic solutions are compared. In the second problem, the localized reactions are nonlinear and the numerical solution is shown to exhibit the correct qualitative features and tend to the theoretical stable equilibrium point of the problem. Two appendices are provided. Appendix A gives details of piecewise polynomial discretization of the BE equations. Appendix B provides expressions for the influence matrices used in the linear convergence analysis.

II. GOVERNING EQUATIONS AND BOUNDARY ELEMENT FORMULATION

A. The Initial-Boundary Value Problem for Linear Diffusion and Localized Nonlinear Reaction

The equations governing the diffusion, adsorption-desorption, and localized reaction are taken to be

$$\frac{\partial \underline{u}}{\partial t} = \underset{\sim}{D}\frac{\partial^2 \underline{u}}{\partial x^2} - \underset{\sim}{\Omega}\underline{u} + \sum_{l=1}^{L} \underline{R}_l(u)\,\delta(x - x_l) + \underline{f} \quad x, x_l \varepsilon (x_0, x_N) \tag{2.1}$$

Here $\underline{u}(x, t) \varepsilon \mathbb{R}^{+s}$ is a vector with positive valued components representing the concentrations of the s different species, $\underline{\underline{D}}$ is a matrix of diffusion coefficients, $\underline{\underline{\Omega}}$ is a matrix representing adsorption-desorption or linear bulk reaction, $\underline{R}_l$ is the rate term due to reactions taking place at the active site x_l, and $\underline{f}(x, t)$ is the incident flux. In this paper we assume that the bulk is homogeneous so that $\underline{\underline{D}}$ and $\underline{\underline{\Omega}}$ are constant, and that the bulk processes are decoupled so that $\underline{\underline{D}}$ and $\underline{\underline{\Omega}}$ are diagonal.

To determine the solution u of (2.1) we prescribe an initial condition

$$\underline{u}(x, 0) = \underline{u}^0(x) \tag{2.2a}$$

and appropriate boundary conditions that may be expressed in the general form:

$$\left(\underline{\underline{\alpha}}_i \frac{\partial}{\partial x} + \underline{\underline{\beta}}_i\right) \underline{u}(x_i, t) = \underline{g}_i(t) \qquad i = 0 \quad \text{and} \quad N \tag{2.2b}$$

Here, as with the bulk, we assume that the boundary conditions are decoupled so that $\underline{\underline{\alpha}}_i$ and $\underline{\underline{\beta}}_i$ are diagonal and $\underline{g}_i$ is a specified function. Hence the only coupling in the equations governing the various species occurs through the reaction term, which is generally nonlinear.

Physically these equations can be used to represent localized reactions that occur at chemically active parallel line-defects on a two-dimensional surface, or they can be used in the modelling of the influence of membrane-bound enzymes in living organisms [1–3]. In the absence of the localized reaction terms $\underline{R}_l$, (2.1)–(2.2) reduces to the classical heat-transfer problem.

B. Boundary Integral Formulation

In this section, the BE formulation of the initial-boundary value problem (2.1)–(2.2) is stated without derivation in view of the fact that the technique is well documented [4–7].

The starting point for the BE formulation is the use of the free-space Green's function associated with the linear partial differential operator in (2.1) to rewrite the solution of (2.1)–(2.2) as an integral equation. Let

$$\gamma(x) = \begin{cases} 0 & x \varepsilon [x_0, x_N] \\ 1 & x \varepsilon (x_0, x_N) \\ \tfrac{1}{2} & x = x_0 \quad \text{or} \quad x_N \end{cases} \qquad \text{then}$$

$$\begin{aligned} \gamma(x)\underline{u}(x, t) = & \int_{x_0}^{x_N} \underline{\underline{G}}(x - \xi, t)\underline{u}^0(\xi)\, d\xi + \int_0^t \int_{x_0}^{x_N} \underline{\underline{G}}(x - \xi, t - \tau)\underline{f}(\xi, \tau)\, d\xi\, d\tau \\ & + \int_0^t \left\{ \left[\underline{\underline{G}}(x - \xi, t - \tau)\underline{\underline{D}} \frac{\partial \underline{u}}{\partial \xi}(\xi, \tau) \right.\right. \\ & \left. - \frac{\partial \underline{\underline{G}}}{\partial \xi}(x - \xi, t - \tau)\underline{\underline{D}}\underline{u}(\xi, \tau) \right] \Bigg|_{\xi = x_0}^{\xi = x_N} \\ & \left. + \sum_{l=1}^{L} \underline{\underline{G}}(x - x_l, t - \tau)\underline{R}_l(u(x_l, \tau)) \right\} d\tau \end{aligned} \tag{2.3}$$

The Green's function $\underset{\sim}{G}(\xi - x, \tau - t)$ is the solution to the following equation

$$\left(\underset{\sim}{D}\frac{\partial^2}{\partial \xi^2} - \underset{\sim}{\Omega} - \underset{\sim}{I}\frac{\partial}{\partial \tau}\right)\underset{\sim}{G}(\xi - x, \tau - t) = -\delta(\xi - x)\delta(\tau - t)\underset{\sim}{I}$$

subject to $\underset{\sim}{G} \to 0$ as $|x| \to \infty$ and the causality condition $\underset{\sim}{G}(x, t) = 0$ if $t < 0$. The explicit expression for $\underset{\sim}{G}$ can be derived using Fourier or Laplace transforms [12, 13]

$$G_{ij}(x, t) = H(t)\frac{\exp[-\Omega_i t - x^2/4D_i t]}{2\sqrt{\pi D_i t}}\delta_{ij} \quad i, j = 1, \ldots, s\,; \; H(t) = \begin{cases} 1 & t \geq 0 \\ 0 & t < 0 \end{cases} \tag{2.4}$$

This Green's function differs from that of the standard diffusion equation through the term $\exp(-\Omega_i t)$ that is due to desorption. The value $\gamma(x_0) = \frac{1}{2}$ is derived by letting $x \to x_0$ from the interior of the interval (x_0, x_N) in (2.3) and evaluating the contribution of the singular kernel $\partial \underset{\sim}{G}/\partial \xi\,(x - \xi, t - \tau)$ over the small interval $(t - \varepsilon, t)$ analytically.

Consider the implications of the integral equation (2.3) for solving a well-posed boundary value problem such as (2.1)–(2.2) in the absence of localized reactions, i.e., $\underset{\sim}{R}_i \equiv 0$. In this case (2.3) is an expression of the solution in terms of quadratures of the prescribed functions $\underset{\sim}{u}^0$ and $\underset{\sim}{f}$ and an integral involving the values of $\underset{\sim}{u}$ and its derivative $\partial \underset{\sim}{u}/\partial x$ at the boundary points x_0 and x_N. If, for example, we were considering Neumann boundary conditions ($\underset{\sim}{\alpha}_i = \underset{\sim}{I}$, $\underset{\sim}{\beta}_i = 0$ in (2.2b)), then all that prevents us from obtaining the solution $\underset{\sim}{u}(x, t)$ directly are the unknown values of $\underset{\sim}{u}$ at x_0 and x_N. If we let $x \to x_0$ and x_N in turn, we obtain two integral equations from which $\underset{\sim}{u}(x_i, t)$ $i = 0, N$ can in principle be found. Once $\underset{\sim}{u}(x_i, t)$ $i = 0, N$ are known, the solution at any point (x, t) can be found by direct quadrature using (2.3). The full variety of boundary value problems as represented by (2.2b) can be solved in an analogous way.

III. CONVERGENCE PROPERTIES OF THE ONE-STEP RECURSION ALGORITHM WHEN USED TO ADVANCE THE SOLUTION OF THE BOUNDARY INTEGRAL FORM OF THE LINEAR DIFFUSION EQUATION

In this section we analyze the convergence properties of a one-step recursion algorithm for advancing the BE solution of the linear diffusion equation in the absence of forcing (i.e., $\underset{\sim}{R}_i = 0$ and $\underset{\sim}{f} = 0$ in (2.1)–(2.2)). We exploit the fact that the one-step recursion algorithm can be expressed in a similar form to explicit finite difference schemes in order to use Lax's Equivalence Theorem [8] to investigate its convergence. We restrict the analysis in this section to the case of a single species $s = 1$ and therefore omit the vector notation used in Section 2.

A. The Piecewise Polynomial One-step Recursion Algorithm for Solving the Boundary Integral Eq. (2.3)

There are a number of different strategies that can be used to obtain a numerical solution of (2.3) [14, 15]. In the piecewise polynomial collocation tech-

nique, the space-time region $[x_0, x_N]x[O,T]$ is divided into cells $[x_e, x_{e+1}]x[t_j, t_{j+1}]$ $e = 0, \ldots, N-1; j = 0, \ldots, M-1$. Over this mesh of space-time cells we construct piecewise polynomial basis functions in terms of which the solution u and specified functions f, g, and u^0 are expanded.

The Volterra form of the time integral in (2.3) can be exploited to arrive at the following one-step recursion time-marching scheme. The solution is carried from one time level t_j to the next $t_{j+1} = t_j + \Delta t_j$ by using (2.3) in which $t = \Delta t_j$, and the solution values at time t_j are regarded as initial values $u^0(x) = u(x,t_j)$. Depending on the prescribed boundary conditions, we solve (2.3) for $u(\xi)$ and/or $(\partial u/\partial \xi)$ (ξ,τ) at the boundaries. Equation (2.3) can then be used to generate $u^{j+1}(x) \equiv u(x, t_{j+1})$, which can be used as initial data for the next step. If we assume that all the time-steps are of the same size, i.e., $\Delta t_j = \Delta t$, then a substantial computational saving can be achieved by a priori generation and storage of the required influence matrices. These influence matrices are formed by integrating the product of the Green's function G and the appropriate piecewise polynomial basis functions. Thus the discretized BE equations can be used to advance the solution by a procedure that involves mainly matrix multiplication (i.e., explicitly). Only terms involving the boundary unknowns have to be solved at every time-step (i.e., treated implicitly). The procedure outlined above is illustrated in Appendix A and influence matrices for piecewise constant and piecewise linear basis functions are given.

The one-step recursion procedure relies heavily on the discretization of the spatial convolution integral of the Green's function and the initial condition (the first integral in Eq. (2.3)) to communicate the effects of preceding the time steps to subsequent time steps. Therefore it can be expected that the error committed in the approximation of this integral will dominate the accumulation of errors in the one-step recursion procedure. The contribution of the approximation of the boundary integrals to the total error is assumed to be subdominant—particularly in the light of the exponential decay of the Green's function in space and the typically small time steps involved in the recursion process. If the extent of the domain is large and the region of interest is far from the boundaries then these assumptions are even more appropriate. We also assume, to facilitate the calculations that follow, that the region of interest is infinite, so that Eq. (A.2) can be written in the form

$$u_m^{j+1} = \sum_{n=-\infty}^{\infty} G_{mn} u_n^j \tag{3.1}$$

The assumption that the domain is infinite is often used in convergence analyses of finite difference schemes. The influence matrices G_{mn} are given in Appendix B for basis functions representing piecewise constant, linear, and quadratic interpolation. In Appendix B, and in the analysis that follows, a uniform spatial mesh with spacing 2a is assumed.

B. Stability of the BE Schemes (3.1)

Because we are analyzing a linear problem, the equation for error amplification is the same as (3.1). Thus we need only check the growth properties of the Fourier modes when the scheme (3.1) is used. To exploit the convolution prop-

erty of the kernel $G_{mn} = G_{m-n}$ in (3.1), we use the following discrete Fourier transform pair [16]:

$$F_\xi(u_N) = \overline{u}(\xi) = 2a \sum_{N=-\infty}^{\infty} e^{-i\xi x_N} u_N; \quad u_N = \frac{1}{2\pi} \int_{-\pi/2a}^{\pi/2a} e^{i\xi x_N} \overline{u}(\xi)\, d\xi$$

We use the following properties associated with this transform pair

(1) Convolution: $\overline{u}(\xi)\overline{v}(\xi) = F_\xi\left\{2a \sum_{k=-\infty}^{\infty} u_k v_{N-k}\right\}$

(2) Parseval's relation:

$$\|u_N\|_2^2 = 2a \sum_{n=-\infty}^{\infty} |u_N|^2 = \frac{1}{2\pi} \int_{-\pi/2a}^{\pi/2a} |\overline{u}(\xi)|^2\, d\xi = \|\overline{u}(\xi)\|_2^2$$

By Parseval's relation we see that to ensure that the solution does not grow as time progresses, we need only ensure that each mode does not grow in time. Using the fact that $G_{mn} - G_{m-n}$ and the convolution property (1) to transform (3.2) we obtain:

$$\overline{u}^{J+1}(\xi) = \frac{1}{2a}\overline{G}(\xi, \Delta t)\overline{u}^J(\xi) = \left\{\frac{1}{2a}\overline{G}(\xi, \Delta t)\right\}^J \overline{u^0}(\xi)$$

Thus none of the modes will grow as $J \to \infty$ provided $|(1/2a)\overline{G}(\xi, \Delta t)| \leq 1$.

By a direct calculation using the definition of the transform $F_\xi\{\ \}$, the expressions for G_{mn} (given in Appendix B), and the triangle inequality we obtain:

$$\left|\frac{1}{2a}\overline{G}(\xi, \Delta t)\right| \leq \operatorname{erf}(\infty) = 1$$

Thus the BE schemes (3.1) are unconditionally stable for all of the piecewise constant, linear and quadratic approximations.

C. Consistency of the BE Schemes (3.1)

In this section it is demonstrated that the piecewise constant and piecewise linear BE schemes are conditionally consistent, while the piecewise quadratic scheme is unconditionally consistent.

To establish consistency [8] it is sufficient to show that the truncation error

$$\frac{\sum_{n=-\infty}^{\infty} G_{mn}(\Delta t, a)U_n^J - U_m^J}{\Delta t} - D\frac{\partial^2 U_m^J}{\partial x^2} \xrightarrow{\Delta t \to 0} 0 \text{ uniformly in } t$$

where U_n^J represents the analytic solution of the differential equation at the nodal point (x_n, t_j).

Proposition 1. The difference scheme (3.1) is consistent with the initial value problem:

$$\frac{\partial u}{\partial t} = D\frac{\partial^2 u}{\partial x^2} \quad x\varepsilon(-\infty, \infty)$$

for any sequence of calculations in which $a \to 0$, $\Delta t \to 0$ in such a way that

$$\Delta t = Ca^{\gamma}$$

where $C > 0$ is some constant and

(i) $o < \gamma < 2$ for the piecewise constant (PWC) and piecewise linear (PWL) schemes

(ii) $o < \gamma < \infty$ for the piecewise quadratic (PWQ) scheme (i.e., unconditionally consistent).

Proof. First we expand U_n around x_m, use the convolution property $G_{mn} = G(|m - n|)$, and use the influence coefficients given in Appendix B to show that

$$\frac{\sum_{n=-\infty}^{\infty} G_{mn}U_n - U_m}{\Delta t} = \frac{4a^2}{\Delta t}\frac{\partial^2 U_m}{\partial x^2} I(\Theta) + \frac{4a^4}{3\Delta t}\frac{\partial^4 U_m}{\partial x^4} J(\Theta) + \ldots \quad (3.3)$$

$$\text{where } \Theta = \frac{2\sqrt{D\Delta t}}{a} \quad \text{and}$$

(a) For the PWC Case.

$$I(\Theta) = \sum_{n=o}^{\infty} n^2 I_{2n-1}^{2n+1} \quad \text{where} \quad I_m^n = \frac{1}{\sqrt{\pi}} \int_{m/\Theta}^{n/\Theta} \exp[-s^2]\,ds$$

$$J(\Theta) = \sum_{n=o}^{\infty} n^4 I_{2n-1}^{2n+1}$$

(b) For the PWL Case.

$$I(\Theta) = \frac{\Theta}{4\sqrt{\pi}}\left\{-1 + 2\sum_{n=0}^{\infty} \exp\left[-4\left(\frac{n}{\Theta}\right)^2\right]\right\} - \sum_{n=0}^{\infty} n(n+1) I_{2n}^{2(n+1)}$$

$$J(\Theta) = \frac{\Theta}{4\sqrt{\pi}}\left\{1 + 2\sum_{n=1}^{\infty} (1 + 6n^2) \exp\left[-4\left(\frac{n}{\Theta}\right)^2\right]\right\}$$

$$- \sum_{n=0}^{\infty} n(n+1)(3n^2 + 3n + 1) I_{2n}^{2(n+1)}$$

(c) For the PWQ Case.

$$I(\Theta) = \Theta^2/16$$

$$J(\Theta) = \frac{1}{12}\sum_{n=0}^{\infty}\left\{[(4n^2 - 1)\{n(2n+1)^3 - 16n^4\} + \frac{\Theta^2}{4}\{(2n+1)^4 - 32n^4\}] I_{2n-1}^{2n+1}\right.$$

$$\left. + (2n+1)^4\left\{(n+1)(2n+3) + \frac{\Theta^2}{4}\right\} I_{2n-1}^{2n+3}\right.$$

$$+\frac{\Theta}{2\sqrt{\pi}}\left[16n^4(2n-1)-3(2n+1)^4\right]\exp\left[\frac{-(2n+1)^2}{\Theta^2}\right]$$
$$+\left\{16n^4(2n+1)-n(2n+1)^4\right\}\exp\left[\frac{-(2n-1)^2}{\Theta^2}\right]$$
$$+\left\{(n+1)(2n+1)^4\right\}\exp\left[\frac{-(2n+3)^2}{\Theta^2}\right]\Bigg]\Bigg\} \tag{3.4}$$

Part (i)

For the PWC and PWL schemes (cases (a) and (b)), the truncation error does not approach 0 for all nonzero finite values of γ without restriction. However, if the mesh is refined, i.e., $a \to 0$, $\Delta t \to 0$ in such a way that $\Delta t = Ca^{\gamma}$ and $o < \gamma < 2$, then in this limit

$$\Theta = \frac{2\sqrt{D\Delta t}}{a} = C'a\left(\frac{\gamma}{2}-1\right) \xrightarrow{a\to 0} \infty .$$

To demonstrate the consistency of these two schemes we need to determine the asymptotic expansions of the sums $I(\Theta)$ and $J(\Theta)$ as $\Theta \to \infty$ for cases (a) and (b).

(a) The PWC Scheme. Consider the asymptotic expansion of $I(\Theta)$. We split the sum into two parts $0 \le n \le [\Theta^{3/2}]$ and $[\Theta^{3/2}] < n$ (here $[\Theta^{3/2}]$ denotes the largest integer less than $\Theta^{3/2}$). Thus

$$I(\Theta) = \frac{1}{\sqrt{\pi}}\sum_{n=o}^{[\Theta^{3/2}]} n^2 \exp\left[-4\left(\frac{n}{\Theta}\right)^2\right]\int_{-1/\Theta}^{1/\Theta}\exp\left[-s^2-4\left(\frac{n}{\Theta}\right)s\right]ds$$
$$+\frac{1}{\sqrt{\pi}}\sum_{n=[\Theta^{3/2}]+1}^{\infty} n^2\int_{(2n-1)/\Theta}^{(2n+1)/\Theta}\exp[-s^2]ds \tag{3.5}$$

The integrals in the first summation on the right side of (3.5) are such that their integrands can be expanded by a Taylor expansion. The contribution of the second summation can be shown to be exponentially small. Integrating the Taylor expansion term by term and interpreting the resulting summations as Riemann sums we have

$$I(\Theta) = \frac{\Theta^2}{16}+\frac{1}{24}+O(1/\Theta^2) \qquad \text{as } \Theta \longrightarrow \infty \tag{3.6a}$$

If we follow a similar procedure with $J(\Theta)$ we obtain

$$J(\Theta) \sim \frac{3\Theta^4}{128} \qquad \text{as } \Theta \longrightarrow \infty$$

If we substitute these expansions into (3.3) we obtain

$$\frac{\sum_{n=-\infty}^{\infty} G_{mn}U_n - U_m}{\Delta t} - D\frac{\partial^2 U_m}{\partial x^2} = \frac{1}{\Delta t}\frac{(2a)^2}{24}\frac{\partial^2 U_m}{\partial x^2}+\ldots+\frac{1}{2}D^2\frac{\partial^4 U_m}{\partial x^4}\Delta t+\ldots \tag{3.7}$$

$$= D\frac{\partial^2 U_m}{\partial x^2} \cdot O(\Delta t^{2/\gamma - 1}, \Delta t) \quad \text{as } \Delta t \longrightarrow 0,\ a \longrightarrow 0\text{: } \Delta t = Ca^{\gamma},\ 0 < \gamma < 2$$

This establishes the consistency of the PWC BEM for the one parameter family of calculations represented by $\Delta t = C \cdot a^{\gamma}$, $0 < \gamma < 2$.

(b) The PWL Scheme. We use a similar procedure as outlined above on the summations involving $I_{2n}^{2(n+1)}$ and interpret the remaining sums as Riemann sums to obtain

$$I(\Theta) = \frac{\Theta^2}{16} + \frac{1}{12} + O\left(\frac{1}{\Theta^2}\right) \quad \text{as } \Theta \longrightarrow \infty \tag{3.6b}$$

and

$$J(\Theta) \sim \frac{3\Theta^4}{128} \quad \text{as } \Theta \longrightarrow \infty$$

The truncation error in this case is of the same order as the PWC case but its leading term is larger by a factor of two. Thus the PWL BE method is also consistent for the one parameter family of calculations represented by $0 < \gamma < 2$. This proves Part (i) of the proposition.

Part (ii)

For the PWQ scheme $I(\Theta) = \Theta^2/16$, so the truncation error only involves terms with the fourth derivative of U_m and higher. Therefore, in order to establish convergence, we must show that $a^4/\Delta t\, J(\Theta) \to 0$ for the sequence of mesh refinement under consideration.

In the case $\Theta \to \infty$, we can perform a similar asymptotic analysis as that given in Part (i). If the mesh is refined in such a way that $0 < \Theta = \text{constant} < \infty$, then $J(\Theta) = \text{constant} < \infty$ since the series converges. If $\Theta \to 0$ as the mesh is refined, then we use Laplace's Method [17] for the asymptotic expansion of series. The results of this analysis are summarized below:

$$J(\Theta) \sim \begin{cases} O(\Theta^4) & \text{as } \Theta \longrightarrow \infty \quad \text{for } 0 < \gamma < 2 \\ \text{constant} & \text{if } 0 < \Theta < \infty \quad \text{for } \gamma = 2 \\ \alpha \exp(-\beta/\Theta^2) & \text{as } \Theta \longrightarrow 0 \quad \text{for } 2 < \gamma < \infty \\ \quad \text{where } \alpha \text{ and } \beta \text{ are constant and } \beta > 0 & \end{cases}$$

In each case $(a^4/\Delta t)\, J(\Theta) \to 0$ so we conclude that the PWQ scheme is consistent for the one-parameter family of meshes represented by $0 < \gamma < \infty$.

D. DISCUSSION OF THE IMPLICATIONS OF THE CONVERGENCE ANALYSIS

Theoretical Implications

If we combine the consistency and stability results of Sections 3 (B) and (C), convergence of the BE method follows from Lax's Equivalence Theorem [8] in

the case of

(i) the PWC and PWL BE method for any sequence of calculations for which $\Delta t,\ a \to 0$ in such a way that $\Delta t = Ca^{\gamma}$ where $0 < \gamma < 2$.

(ii) the PWQ BE method for any sequence of calculations in which $\Delta t,\ a \to 0$, in which case $\Delta t = Ca^{\gamma}$ where $0 < \gamma < \infty$.

We see that for the PWC and PWL schemes the crucial property of a successful mesh sequence is that $\Theta \to \infty$ as $\Delta t,\ a \to 0$ to ensure that the asymptotic expansions for $I(\Theta)$ and $J(\Theta)$ are valid. If, for a given sequence of meshes, a set of difference equations is not consistent with the differential equation they approximate, then in this limit the difference equations do not reduce to the given differential equation. In the above proposition the case $\gamma = 2$ is excluded as the PWC and PWL BE methods are then not consistent because in such a mesh sequence $\Theta = 2(\sqrt{D\Delta t}/a) = \text{constant} < \infty$. Surprisingly we see from Figure 1 that for $\Theta > 2$, the asymptotic expansion (3.6a) already gives a good approximation to $I(\Theta)$. From (3.7) we see that for such a mesh sequence, the BE difference equations (3.1) approximate the differential equations:

$$\frac{\partial u}{\partial t} = D\left(1 + \frac{2}{3\Theta^2}\right)\frac{\partial^2 u}{\partial x^2} \text{ in the PWC case}$$

and (3.8)

$$\frac{\partial u}{\partial t} = D\left(1 + \frac{4}{3\Theta^2}\right)\frac{\partial^2 u}{\partial x^2} \text{ in the PWL case}$$

Since Θ = constant for all meshes in the sequence represented by $\gamma = 2$, the

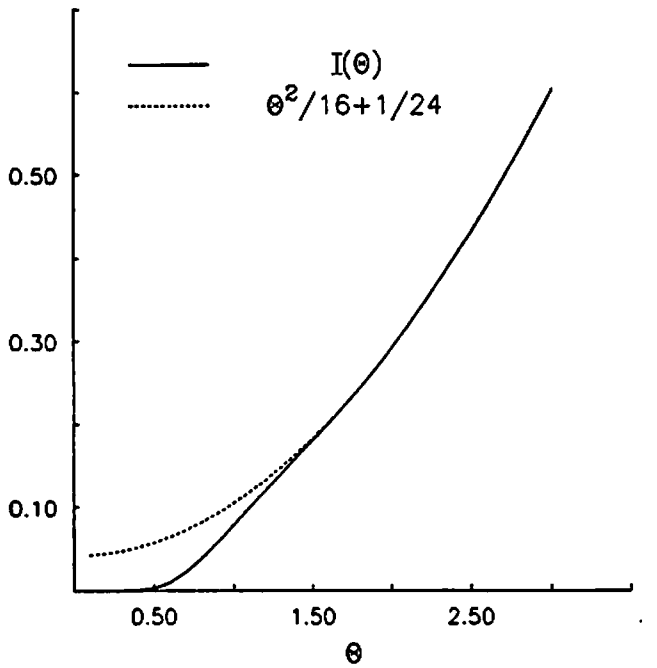

FIG. 1. Comparison of $I(\Theta)$ and its asymptotic expansion as $\Theta \to \infty$, which is given in (3.6a). The close agreement for $\Theta > 2$ is clear.

BE difference equations will approximate a diffusion equation in which the diffusion coefficient is consistently too large. This phenomenon of "numerical diffusion" will be illustrated in Section 3(E). The case $0 < \gamma < 2$ considered in the proposition may be interpreted as a family of meshes in which the diffusion coefficient is initially too large, but in which the correct value is achieved as the mesh is refined and $\Theta \to \infty$. We now decrease the size of Δt relative to a further than $\gamma = 2$ by choosing $\gamma > 2$. In this case $\Theta \to 0$ as $\Delta t \to 0$, and the BE difference equations approximate the differential equation $(du/dt) = 0$. The conditional consistency of the PWC and PWL schemes thus prohibits small time-steps, i.e., $\gamma \geq 2$, while consistency places no restriction on how large Δt can be made relative to a $0 < \gamma < 2$. This is significant from a computational point of view as it allows the solution to be advanced in time with fewer and larger time-steps. This is in contrast to explicit finite difference schemes where Δt cannot exceed an upper value proportional to a^2.

The excess diffusion observed for the PWC and PWL BE schemes when $2 \leqslant \gamma < \infty$, does not occur for the PWQ BE scheme which yields a sequence of convergent difference equations irrespective of the relative sizes of the time and spatial meshing.

Practical Implications

In contrast to the hypothetical sequence of meshes constructed for the above theoretical analysis, we are in practice confronted with the issue of deciding on an appropriate algorithm and mesh for a given problem. The above analysis can also be used to shed light on such a choice.

First, for the PWC and PWL BE schemes a minimal consistency requirement of a mesh is that the asymptotic expansion (3.6) should be valid. From Fig. 1 it can be seen that for the PWC scheme $\Theta > 2$ is sufficient to ensure consistency. If $(1/\Theta^2) \ll 1$ then from (3.8) we can expect the BE method to provide good approximations provided Δt is not too large. Also if we examine the first and second terms given explicitly on the right of (3.7) we observe that for a given spatial mesh size a we can predict the existence of an optimal time-step. This will be determined by the value of Δt for which these two terms are equal. Since these two terms depend on the derivatives of the solution, an a priori estimate of the optimal time-step is not possible.

E. Numerical Illustration of Convergence Properties

In this section we illustrate the convergence properties that we established in Sections (B) through (D) by means of a simple example.

$$\frac{\partial u}{\partial t} = D\frac{\partial^2 u}{\partial x^2} \qquad x\varepsilon(0, 1)$$

We consider the scalar initial-boundary value problem [18]

$$u(x, 0) = \begin{cases} 2x & 0 \leq x \leq \frac{1}{2} \\ 2(1 - x) & \frac{1}{2} < x \leq 1 \end{cases} \tag{3.9}$$

$$u(0, t) = 0 = u(1, t)$$

The analytic solution to this problem can be obtained by separation of variables and is given by:

$$u(x,t) = \frac{8}{\pi^2} \sum_{n=1}^{\infty} \frac{1}{n^2} \sin\left(\frac{n\pi}{2}\right) \sin(n\pi x) \exp(-Dn^2\pi^2 t)$$

A sequence of runs was performed for a variety of time-steps $\Delta t = 0.1$, 0.05, 0.025, 0.01, 0.005, and 0.001. In each case 10 spatial cells were used (i.e., $2a = 0.1$) and $D = 1.0$. Figure 2 shows the PWC BE solutions at $t = 0.1$ in which various time-steps are used. The analytic solution is also plotted for

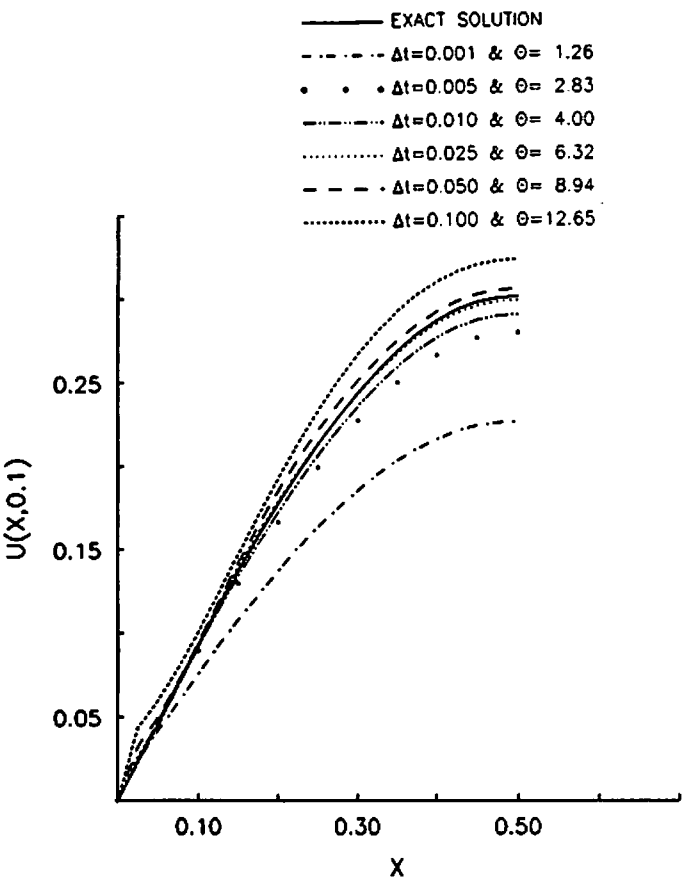

FIG. 2. Exact and Piecewise Constant BE solutions at $t = 0.1$ using $a = 0.05$ and various time-steps. (a) $\Delta t = 0.001$ so $\Theta = 1.26$: clear lack of consistency characterized by excess diffusion even greater than that predicted by (3.8). (b) $\Delta t = 0.005$ so $\Theta = 2.8$: lack of consistency but the excess diffusion is exactly as predicted by (3.8) because Θ satisfies the minimal consistency requirement $\Theta > 2$. (c) $\Delta t = 0.01$ so $\Theta = 4.0$: same as in (b). (d) $\Delta t = 0.025$ so $\Theta = 6.32$: no lack of consistency and time-step is nearly optimal. (e) $\Delta t = 0.05$ so $\Theta = 8.9$: no lack of consistency but degradation in accuracy due to the boundary interpolation scheme for such a large time-step. (f) $\Delta t = 0.1$ so $\Theta = 12.6$: same as in (e), still no instability even for such a large time-step.

comparison. The following trends are observed:

$\Delta t = 0.001$, $\Theta = 1.26$: There is a lack of consistency characterized by an excessive amount of diffusion of the numerical solution. In this case there is even more excess diffusion than predicted by (3.8) owing to the fact that for such a low value of $\theta < 2$, the mesh does not satisfy the minimal consistency requirement of validity of the asymptotic expansion (3.6a) (see Figure 1).

$\Delta t = 0.005$–0.01, $\Theta = 2.8$–4: These numerical solutions also exhibit a lack of consistency characterized by excessive diffusion. However, these two meshes do satisfy the minimal consistency requirement, and the excess diffusion in each case corresponds to that predicted by (3.8).

$\Delta t = 0.025$, $\Theta = 6.32$: In this case the excess diffusion is negligible and the time-step is nearly optimal.

$\Delta t = 0.05$–0.01: As in the case $\Delta t = 0.025$ the excess diffusion is negligible. However, in these two examples a degradation in accuracy is observed. This is a direct result of the large time-step that has been used. As mentioned in Section D, a greater accuracy for large time-steps can be achieved by using higher degree time-interpolation on the boundaries. This improvement can be seen in Fig. 3 in which linear time-interpolation is used.

In Fig. 3 the PWL BE solutions at $t = 0.1$ for the selected range of time-steps are presented. A similar degradation in the BE solution is observed for small time-steps. In fact, for time-steps $\Delta t = 0.01$ and $\Delta t = 0.005$ the excess diffusion for the PWL case is exactly double that of the PWC case. This agrees precisely with the theoretical values of the excess diffusion for the PWC and PWL schemes given in (3.8). For the larger time-steps $\Delta t = 0.05$ and $\Delta t = 0.1$, the degradation in accuracy is less marked when the PWL time-interpolation is used than when PWC interpolation with endpoint collocation is used (compare the solutions $\Delta t = 0.1$ in Figs. 2 and 3). This insight can be used to determine the most appropriate algorithm for a given problem.

In Fig. 4 the PWQ BE solutions at $t = 0.1$ for the selected range of time-step are presented. In this case there is no excess diffusion associated with loss of consistency when small time-steps are used. In fact, the solution improves as the time-steps are decreased and become virtually indistinguishable from the exact solution for $\Delta t \leq 0.025$. This confirms the results of the convergence analysis of Sections B through D. As was the case for the PWC and PWL schemes, the PWQ solution also degrades as the time-step is increased, e.g., $\Delta t = 0.1$, due to boundary discretization. The sizes of the spatial cells ($2a = 0.1$) were kept the same as those of the PWC and PWL schemes in spite of the fact that the number of spatial mesh points was in effect doubled. This was done so that the numerical results were compatible with the convention adopted in the convergence analysis. To be fair to the other schemes, a comparison should be made between solutions involving the same number of degrees of freedom. Such a PWQ solution was determined in which $2a = 0.2$. The coarse mesh PWQ solution showed only a slight degradation compared to the fine mesh PWQ solution and did not display the phenomenon of numerical diffusion. This is consistent with the predictions of the convergence analysis. However, since the objective here is to illustrate the convergence properties rather than to provide a direct accuracy comparison, these results are omitted.

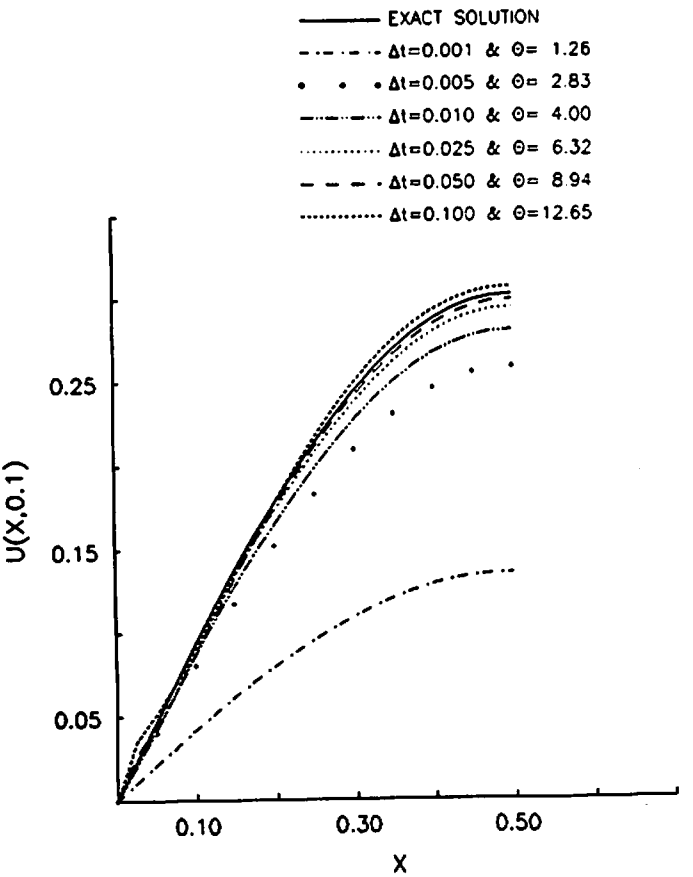

FIG. 3. Exact and Piecewise linear BE solutions at $t = 0.1$ using $a = 0.005$ and for the same time-steps as in Fig. 2. The same trends as in Fig. 2 are observed but in this case twice as much excess diffusion occurs for the small time-steps $\Delta t = 0.005$ and 0.01. Also for the large time-steps $\Delta t = 0.05$ and 0.1 there is less degradation in accuracy because of the more accurate boundary interpolation scheme.

Finally, in Figs. 2 to 4 there is no hint of numerical instability even when large time-steps are used. This confirms the unconditional stability that was established in Section B for all the BE schemes. This behavior is distinct from that of explicit difference schemes such as the explicit Euler scheme with central differences [18]. This scheme would experience severe instability problems for any time-steps larger than $\Delta t = 0.005$, while all the BE schemes are still stable when $\Delta t = 0.1$ and larger. The close correspondence between the theoretical predictions of the convergence analysis and the numerical results validates the assumption that the dominant accumulation of errors in the one-step recursion procedure is due to the approximation of the spatial convolution integral of the Green's function and the initial condition.

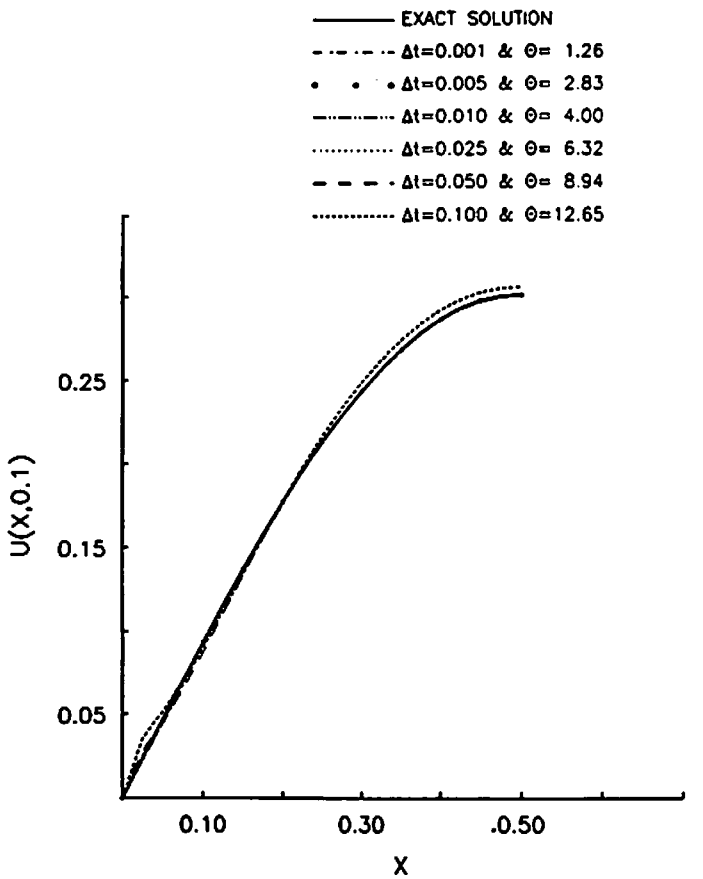

FIG. 4. Exact and Piecewise quadratic BE solutions at $t = 0.01$ using $a = 0.05$ and the same range of time-steps as in Fig. 2. Consistent with the unconditional convergence of this scheme, there is no excess diffusion observed. There is only a slight degradation in accuracy observed for $\Delta t = 0.1$ due to the degradation in accuracy of the boundary interpolation scheme.

IV. CONVERGENCE OF AN EXPLICIT PIECEWISE LINEAR CARATHEODORY ITERATION ALGORITHM TO ADVANCE THE SOLUTION AT LOCALIZED REACTION SITES

In this section we consider the convergence of an explicit algorithm to advance the solution at a localized reaction site forward in time by means of Caratheodory iteration combined with piecewise linear interpolation. To be able to focus on the accumulation of errors when the piecewise linear Caratheodory iteration (PLCI) procedure is used to advance the solution, we make some simplifying assumptions. In this case (2.3) reduces to a nonlinear, singular Volterra integral equation in time. This equation can either be regarded as a model prob-

lem that retains the dominant features of the original problem, or a special case of (2.3) that is realized for special regions. We give some examples in which (2.3) reduces to the model problem.

To prove the convergence of the time discretization scheme based on piecewise linear collocation, we exploit the techniques used by Miller [11] to analyze the existence and uniqueness of nonlinear singular Volterra integral equations. While this approach does not yield a completely general theory applicable to all problems, it demonstrates that the piecewise linear collocation technique does provide a convergent scheme in this nonlinear environment. Finally, the performance of the piecewise linear collocation scheme is illustrated in two numerical examples.

A. Model Problem

We consider a class of problems in which the active sites are located in a region remote from the boundaries. In this case the contribution of the boundary terms in (2.3) are assumed to be negligibly small. Furthermore, we assume that we have a problem for which the solution value $\underset{\sim}{u}(x_l, t)$ at each of the active sites is identical, i.e., $\underset{\sim}{u}(x_1, t) = \underset{\sim}{u}(x_2, t) = \cdots = \underset{\sim}{u}(x_L \cdot t)$. This situation occurs in the case of a single active site in an infinite domain or in the case of an infinite periodic array of active sites. This symmetry is not restricted to one-dimensional problems. For example, in two dimensions we can envision an active circular ring, or in three dimensions an active spherical shell. Each of these problems is essentially one-dimensional due to symmetry. We now write down the integral eq. (2.3) in the special case when the field point x coincides with one of these active sites. In this case the integral Eq. (2.3) reduces to the form:

$$\underset{\sim}{u}(t) = \underset{\sim}{F}(t) + \int_0^t \underset{\approx}{g}(t - \tau)\underset{\sim}{R}(\underset{\sim}{u}(\tau))\, d\tau \tag{4.1}$$

Here the first two terms of (2.3) have been absorbed into the term $\underset{\sim}{F}(t)$, the reactions taking place at each of the active sites are assumed to be indentical, i.e., $\underset{\sim}{R}_l \equiv \underset{\sim}{R}$ for all l, and the kernel $\underset{\approx}{g}$ for the various problems is as follows:

(a) a single active site in an infinite domain:

$$g_{ij}(t) = H(t)\frac{\exp(-\Omega_i t)}{(4\pi D_i t)^{1/2}}\delta_{ij} \tag{4.2a}$$

(b) a periodic array of active sites a distance h apart:

$$g_{ij}(t) = H(t)\left\{\sum_{n=-\infty}^{\infty} \exp\left[-\frac{n^2h^2}{4D_i t}\right]\right\}\frac{\exp(-\Omega_i t)}{(4\pi D_i t)^{1/2}}\delta_{ij} \tag{4.2b}$$

(c) an active circular ring of radius a:

$$g_{ij}(t) = H(t)\,\frac{a}{4\pi D_i t}\exp\left[-\frac{a^2}{2D_i t} - \Omega_i t\right] I_0\left(\frac{a^2}{2D_i t}\right) \tag{4.2c}$$

Here $H(t)$ is the Heavyside function defined in (2.4) and I_0 is the zeroth order modified Bessel function of the first kind.

To develop the theory that follows, we shall require that $\underset{\sim}{F}$, $\underset{\sim}{g}$, and $\underset{\sim}{R}$ satisfy a number of properties that we now state and motivate:

(P1) $\underset{\sim}{F}:[0,T] \to \mathbb{R}^s$ is continuous:

Motivation. Provided $u_i^0(x)$ is continuous on $(-\infty,\infty)$ it can be shown [11] that $\underset{\sim}{F}(t)$ is continuous for all $t \geq 0$.

(P2) $\underset{\sim}{g}:[0,T] \to \mathbb{R}^s \times \mathbb{R}^s$ is an element of $L^1([0,T], \mathbb{R}^s \times \mathbb{R}^s)$:

Motivation. We consider each of the above cases (4.2a–c) in turn.

(a) Trivial

(b) The simple estimate

$$\left| \sum_{n=-\infty}^{\infty} \exp\left[-\frac{n^2h^2}{4Dt} \right] \right| \leq 1 + \frac{(4\pi Dt)^{1/2}}{h}$$

and an application of the Lebesgue dominated convergence theorem yields the desired result.

(c) as $t \to 0$, $g_{ij}(t) \sim \delta_{ij}/(16\pi^3 D_i t)^{1/2}$ so that $\underset{\sim}{g} \in L^1([0,T], \mathbb{R}^s)$

We note that provided $\Omega_i \neq 0$, $i = 1, \ldots, s$ (P2) holds for all $T < \infty$,

(P3) $\underset{\sim}{R}:\mathbb{R}^s \to \mathbb{R}^s$ is assumed to be a continuous function:

Motivation. In isothermal reaction kinetics $\underset{\sim}{R}$ is often assumed to be analytic, and the corresponding Taylor Series is commonly truncated and only second- or third-order terms retained.

B. Piecewise Linear Caratheodory Iterates

In this section we define a Caratheodory iteration scheme that is based on piecewise linear interpolation. The scheme involves advancing across a finite time interval $[0,b] \subseteq [0,T]$ an approximate solution that uses piecewise linear interpolation and collocation at a finite number of nodal points. These Caratheodory iterates differ from those used by Miller [11] in that only a finite number of degrees of freedom are needed for each piecewise linear iterate. In contrast, those used by Miller involve determining a function for each iterate, which essentially involves an infinite number of degrees of freedom. However, since our task is one of approximation, the piecewise linear Caratheodory iterates (PLCI) are better suited to our purposes than those of Miller, who was interested in questions of existence. These PLCI have the useful property that the approximate solution is marched in an explicit fashion so that a system of nonlinear equations do not have to be solved every time-step.

Given $J \in \mathbb{Z}$ we partition the bounded interval $[0,b]$ into subintervals of length $\varepsilon_J = b/J$. Let $X = (C[0,b], |\cdot|_\infty)$ be the Banach space of continuous functions mapping $[0,b]$ to $\mathbb{R}$ and let $|\cdot|_\infty$ be a norm constructed by combining some vector norm on $\mathbb{R}^s$ with the sup norm on $[0,b]$. Let X_J be the $S(J+1)$ dimensional subspace of X comprising the piecewise linear functions defined on the subintervals of length ε_J. Let $L_J : X \to X_J$ define the projection operator that maps a function $u \in X$ onto its piecewise linear interpolant $L_J u \in X_J$. We now

define the PLCI for (4.1) as follows:

$$\left.\begin{aligned} \psi_j(t) &= L_j\underset{\sim}{F}(t) \qquad 0 \le t \le \varepsilon_j \\ \psi_j(t) &= L_j\underset{\sim}{F}(t) + \int_0^{t-\varepsilon_j} \underset{\approx}{g}(t - \varepsilon_j - \tau)L_j\underset{\sim}{R}(\psi_j(\tau))\,d\tau; \quad \varepsilon_j < t < b \end{aligned}\right\} \tag{4.3}$$

Thus we can define a sequence $\{\psi_j(t)\}_{j=1}^{\infty}$ of PLCI of (4.1).

C. Convergence of the PLCI to a Solution of (4.1)

In this section we prove that the PLCI converge uniformly on $[0,b]$ to a continuous solution of (4.1). The theory holds for a finite time interval $[0,b]$, the size of which is determined by on $\underset{\sim}{F}$, $\underset{\approx}{g}$ and $\underset{\sim}{R}$. The interval of convergence $[0,b]$ for the piecewise Caratheodory iterates defined in (4.3) is identical to the interval of existence guaranteed by the Miller theory. We have chosen not to place additional restrictions on $\underset{\sim}{R}$ that will guarantee uniqueness because it is often of interest to obtain an approximate solution of (2.1) in the regime of multiple solutions.

Theorem 1. Let $\underset{\sim}{F}$, $\underset{\approx}{g}$, and $\underset{\sim}{R}$ satisfy conditions (P1), (P2), and (P3) respectively, then there exists a $b\varepsilon(0,T]$ and a subsequence of PLCI defined by (4.3), which converge uniformly on $[0,b]$ to a continuous solution of (4.1).

Restrictions on the interval of convergence:

$$\text{(i)} \quad \text{let } M_0 = \max_{t\varepsilon[0,T]} |L_j\underset{\sim}{F}(t)| \tag{4.4a}$$

$$\text{(ii)} \quad \text{let } M_1 = \max_{\substack{x\varepsilon\mathbb{R}^s \\ |x|\le 2M_0}} |\underset{\sim}{R}(x)| \tag{4.4b}$$

then choose the number b such that $0 < b < T$ and such that

$$M_1 \int_0^b |\underset{\approx}{g}(s)|\,ds < M_0 \tag{4.4c}$$

Notice that we have let $|\cdot|$ denote the vector norm on $\mathbb{R}^s$ that is used in the definition of $|\cdot|_\infty$, and $|\underset{\approx}{g}(s)|$ denote a consistent matrix norm of $\underset{\approx}{g}$ induced by the vector norm $|\cdot|$.

We prove theorem 1 using the following five lemmas:

Lemma 1. Let $\underset{\sim}{F}\ \varepsilon\ X = (C[0,B], |\cdot|_\infty)$ then the sequence $\{L_j\underset{\sim}{F}\}_{j=1}^{\infty}$ where $L_j\underset{\sim}{F}\ \varepsilon\ X_j$ is equicontinuous on $[0,B]$

Proof. Let $t\varepsilon[0,B]$ and $h{:}t + h\varepsilon[0,B]$. By the triangle inequality we have $|L_j\underset{\sim}{F}(t+h) - L_j\underset{\sim}{F}(t)| \le |L_j\underset{\sim}{F}(t+h) - \underset{\sim}{F}(t+h)| + |\underset{\sim}{F}(t+h) - \underset{\sim}{F}(t)| + |L_j\underset{\sim}{F}(t) - \underset{\sim}{F}(t)|$. Let $\varepsilon > 0$ be given. Since $L_j\underset{\sim}{F} \xrightarrow{J\to\infty} \underset{\sim}{F}$ in the sup norm on $[0,b]$ there exists an $N(\varepsilon)$:

$$J \ge N(\varepsilon) \Rightarrow |L_j\underset{\sim}{F}(\tau) - \underset{\sim}{F}(\tau)| < \varepsilon/3 \quad \text{for all } \tau\varepsilon\,[0,B]$$

Now since $L_j\underset{\sim}{F}$ are continuous there exists for each $J = 1,\ldots,N(\varepsilon) - 1$ a $\delta_j(\varepsilon) > 0$:

$$|h| < \delta_J(\varepsilon) \Rightarrow |L_J \underset{\sim}{F}(t+h) - L_J \underset{\sim}{F}(t)| < \varepsilon$$

Finally since $\underset{\sim}{F}$ is continuous there exists a $\delta_F(\varepsilon) > 0$:

$$|h| < \delta_F(\varepsilon) \Rightarrow |\underset{\sim}{F}(t+h) - \underset{\sim}{F}(t)| < \varepsilon/3$$

We now choose $\delta = \min\{\delta_1(\varepsilon), \ldots, \delta_{N(\varepsilon)-1}(\varepsilon), \delta_F(\varepsilon)\}$ for which

$$|h| < \delta \Rightarrow |L_J \underset{\sim}{F}(t+h) - L_J \underset{\sim}{F}(t)| < \varepsilon \text{ independent of } J$$

QED

Lemma 2. The sequence $\{\psi_J(t)\}$ is uniformly bounded on some subinterval $[0,b] \subset [0,T]$

Proof. The proof is by induction on the subintervals into which $[0,b]$ is divided when the Caratheodory iterates are set up in (4.3).

$t\varepsilon[0, \varepsilon_J]$:

$$|\underset{\sim}{\psi}_J(t)| = |L_J \underset{\sim}{F}(t)| \le M_0 \le 2M_0 \qquad \text{by (4.4a).}$$

$t\varepsilon(\varepsilon_J, 2\varepsilon_J]$:

$$\begin{aligned} |\underset{\sim}{\psi}_J(t)| &\le |L_J \underset{\sim}{F}(t)| + \int_0^{t-\varepsilon_J} |\underset{\sim}{g}(t - \varepsilon_J - \tau)|\,|L_J \underset{\sim}{R}(\psi_J(\tau))|\,d\tau \\ &\le M_0 + M_1 \int_0^{t-\varepsilon_J} |\underset{\sim}{g}(t - \varepsilon_J - \tau)|\,d\tau \qquad \text{by (4.4a,b)} \\ &\le 2M_0 \qquad \text{by (4.4c)} \end{aligned}$$

This process can be continued over the whole interval $[0,b]$.
Thus $|\psi_J(t)| \le 2M_0$ for all $t\varepsilon[0,b]$ and for all J.

QED

Lemma 3. The sequence $\{\underset{\sim}{\psi}_J\}_{J=1}^{\infty}$ is equicontinuous at any point $t\varepsilon[0,b]$.

Proof. $t = 0$: From (4.3) it follows directly that

$$\underset{\sim}{\psi}_J(h) - \underset{\sim}{\psi}_J(0) = L_J \underset{\sim}{F}(h) - \underset{\sim}{F}(0) \quad \text{for} \quad 0 \le h \le \varepsilon_J$$

$$\underset{\sim}{\psi}_J(h) - \underset{\sim}{\psi}_J(0) = L_J \underset{\sim}{F}(h) - \underset{\sim}{F}(0) + \int_0^{h-\varepsilon_J} \underset{\sim}{g}(h - \varepsilon_J - \tau) L_J(\underset{\sim}{\psi}_J(\tau))\,d\tau$$

$$\varepsilon_J < h < b$$

Let $\bar{h} = \max\{0, h - \varepsilon_J\}$; then combining the above two equations we have

$$\begin{aligned} |\underset{\sim}{\psi}_J(h) - \underset{\sim}{\psi}_J(0)| &\le |L_J \underset{\sim}{F}(h) - L_J \underset{\sim}{F}(0)| + \int_0^{\bar{h}} |\underset{\sim}{g}(\bar{h} - \tau)|\,|L_J \underset{\sim}{R}(\underset{\sim}{\psi}_J(\tau))|\,d\tau \\ &\le |L_J \underset{\sim}{F}(h) - L_J \underset{\sim}{F}(0)| + M_1 \int_0^{\bar{h}} |\underset{\sim}{g}(s)|\,ds \qquad \text{by Lemma 2} \end{aligned}$$

Now since $\{L_J \underset{\sim}{F}\}_{J=1}^{\infty}$ is equicontinuous by Lemma 1, the right-hand side approaches 0 as $h \to 0$ for all J. So the result is established for $t = 0$.

$0 < t \le b$,: Choose J such that $\varepsilon_J < t \le \varepsilon_{J-1}$ and pick h small enough that

$\varepsilon_j < t + h < b$. If $j \geq J$, then

$$\psi_j(t+h) - \psi_j(t) = L_j\underset{\sim}{F}(t+h) - L_j\underset{\sim}{F}(t) + \int_0^{t-\varepsilon_j} \{\underset{\sim}{g}(t+h-\varepsilon_j-s) - \underset{\sim}{g}(t-\varepsilon_j-s)\}L_j\underset{\sim}{R}(\psi_j(s))\,ds + \int_{t-\varepsilon_j}^{t+h-\varepsilon_j} \underset{\sim}{g}(t+h-\varepsilon_j-s)L_j\underset{\sim}{R}(\psi_j(s))\,ds$$

thus

$$\begin{aligned} |\psi_j(t+h) - \psi_j(t)| &\leq |L_j\underset{\sim}{F}(t+h) - L_j\underset{\sim}{F}(t)| + M_1\int_0^{t-\varepsilon_j} |\underset{\sim}{g}(s+h) - \underset{\sim}{g}(s)|\,ds \\ &\quad + M_1\int_0^h |\underset{\sim}{g}(s)|\,ds \\ &\leq |L_j\underset{\sim}{F}(t+h) - L_j\underset{\sim}{F}(t)| + M_1\int_0^t |\underset{\sim}{g}(s+h) - \underset{\sim}{g}(s)|\,ds \\ &\quad + M_1\int_0^h |\underset{\sim}{g}(s)|\,ds \end{aligned} \tag{4.5}$$

Since $\{L_j\underset{\sim}{F}\}_{j=0}^{\infty}$ are equicontinuous by Lemma 1, the first term on the right of (4.5) approaches 0 as $h \to 0$ for all j. Since $\underset{\sim}{g}$ is an L^1 function we can use the Lebesgue dominated convergence theorem to show that the second term on the right of (4.5) approaches 0 as $h \to 0$. Since $\psi_1, \ldots, \psi_{j-1}$ are only finite in number and continuous, given an $\varepsilon > 0$ it is thus possible to choose a $\delta(\varepsilon) > 0$ such that $|h| < \delta(\varepsilon) \Rightarrow |\psi_j(t+h) - \psi_j(t)| < \varepsilon$ for all j.

QED

The Arzela-Ascoli Theorem [19] combined with Lemmas 2 and 3 implies that $\{\psi_j\}_{j=1}^{\infty}$ has a subsequence $\{\psi_{j_K}\}$ that converges uniformly on $[0,b]$ to a continuous limit function $\psi(t)$. We next show that the subsequence of $\{L_j\psi_j\}_{j=1}^{\infty}$ corresponding to $\{\psi_{j_K}\}$ also converges uniformly to $\psi(t)$.

Lemma 4. Let $\{\underset{\sim}{h}_n(t)\}_{n=1}^{\infty}$ be a sequence of continuous functions that converge uniformly to a continuous limit function $\underset{\sim}{h}(t)$, then $L_n\underset{\sim}{h}_n(t) \varepsilon X_n$ converges uniformly to $\underset{\sim}{h}(t)$.

Proof. Since $\underset{\sim}{h}(t) \varepsilon X$, we know that the sequence $\{L_n\underset{\sim}{h}\}_{n=1}^{\infty}$ of piecewise linear interpolants converge uniformly to $\underset{\sim}{h}$. Thus given an $\varepsilon > 0$ there exists an $M(\varepsilon)$:

$$m > M(\varepsilon) \Rightarrow |L_m\underset{\sim}{h} - \underset{\sim}{h}|_\infty < \varepsilon$$

Now since $\underset{\sim}{h}_n$ converges to $\underset{\sim}{h}$ uniformly there exists an $N(\varepsilon)$:

$$n > N(\varepsilon) \Rightarrow |\underset{\sim}{h}_n - \underset{\sim}{h}|_\infty < \varepsilon$$

Now using the triangle inequality

$$|L_n\underset{\sim}{h}_n - \underset{\sim}{h}|_\infty \leq |L_n(\underset{\sim}{h}_n - \underset{\sim}{h})|_\infty + |L_n\underset{\sim}{h} - \underset{\sim}{h}|_\infty$$

Now if we choose $n > N' = \max\{M(\varepsilon), N(\varepsilon)\}$ then it follows that $|\underset{\sim}{h}_n - \underset{\sim}{h}|_\infty < \varepsilon$. Combining this with the fact that the function $\underset{\sim}{h}_n - \underset{\sim}{h}$ is continuous, and using piecewise linear basis functions to expand $L_n(h_n - h)$, we can derive the estimate

$$|L_n(\underset{\sim}{h}_n - \underset{\sim}{h})|_\infty \leq |\underset{\sim}{h}_n - \underset{\sim}{h}|_\infty < \varepsilon$$

Thus $n > N' \Rightarrow |L_n\underset{\sim}{h}_n - \underset{\sim}{h}|_\infty < \varepsilon$

QED

Lemma 5. There exists a subsequence of $\{\underset{\sim}{\psi}_j(t)\}_{j=1}^\infty$ that converges uniformly on $[0,b]$ to a solution $\underset{\sim}{\psi}(t)$ of (4.1).

Proof. Let $\{\underset{\sim}{\psi}_n(t)\}_{n=1}^\infty$ denote the elements of the subsequence of $\{\underset{\sim}{\psi}_{j_K}(t)\}_{j=1}^\infty$, which by the Arzela Ascoli Theorem converge uniformly to the continuous limit function $\underset{\sim}{\psi}(t)$.

$t = 0$:
$$\underset{\sim}{\psi}(0) = \lim_{n\to\infty} \underset{\sim}{\psi}_n(t) = \lim_{n\to\infty} \underset{\sim}{F}(0) = \underset{\sim}{F}(0)$$

$0 < t \leq b$:

$$\text{(i)} \quad L_n\underset{\sim}{F}(t + (b/n)) \longrightarrow \underset{\sim}{F}(t) \quad \text{as } n \longrightarrow \infty$$

$$\text{(ii)} \quad \left|\int_0^t \underset{\sim}{g}(t - s)[L_n\underset{\sim}{R}(\underset{\sim}{\psi}_n(s)) - \underset{\sim}{R}(\underset{\sim}{\psi}(s))]\,ds\right| \leq \max_{\tau\in[0,b]}|L_n\underset{\sim}{R}(\underset{\sim}{\psi}_n(\tau)) - \underset{\sim}{R}(\underset{\sim}{\psi}(\tau))|\int_0^b |\underset{\sim}{g}(s)|\,ds \tag{4.6}$$

Since $\underset{\sim}{\psi}_n \longrightarrow \underset{\sim}{\psi}$ uniformly and $\underset{\sim}{R}$ is continuous, it follows that the sequence $\underset{\sim}{R}(\underset{\sim}{\psi}_n(t))$ converges uniformly to $\underset{\sim}{R}(\underset{\sim}{\psi}(t))$ on $[0,b]$. Applying Lemma 4 it follows that $L_n\underset{\sim}{R}(\underset{\sim}{\psi}_n) \longrightarrow \underset{\sim}{R}(\underset{\sim}{\psi})$ uniformly. Thus the right-hand side of (4.6) approaches 0 as $n \longrightarrow \infty$ since $\int_0^b |\underset{\sim}{g}(s)|\,ds < \infty$ by (P2).

$$\text{(iii)} \quad \underset{\sim}{\psi}_n(t + (b/n)) \longrightarrow \underset{\sim}{\psi}(t) \quad \text{as } n \longrightarrow \infty$$

This follows from the inequality

$$|\underset{\sim}{\psi}_n(t + (b/n)) - \underset{\sim}{\psi}(t)| \leq |\underset{\sim}{\psi}_n(t + (b/n)) - \underset{\sim}{\psi}_n(t)| + |\underset{\sim}{\psi}_n(t) - \underset{\sim}{\psi}(t)| \tag{4.7}$$

The first term on the right of (4.7) can be made arbitrarily small as $n \longrightarrow \infty$ by exploiting the equicontinuity of $\{\underset{\sim}{\psi}_n\}$, while the second can also be made arbitrarily small since $\underset{\sim}{\psi}_n \longrightarrow \underset{\sim}{\psi}$ as $n \longrightarrow \infty$.

Combining (i) through (iii) and using (4.3), we have

$$\begin{aligned}\underset{\sim}{\psi}(t) &= \lim_{n\to\infty} \underset{\sim}{\psi}_n(t + (b/n)) \\ &= \lim_{n\to\infty}\left\{L_n\underset{\sim}{F}(t + (b/n)) + \int_0^t \underset{\sim}{g}(t - \tau)L_n\underset{\sim}{R}(\underset{\sim}{\psi}_n h(\tau))\,d\tau\right\} \\ &= \underset{\sim}{F}(t) + \int_0^t \underset{\sim}{g}(t - \tau)\underset{\sim}{R}(\underset{\sim}{\psi}(t))\,d\tau\end{aligned}$$

which shows that $\underset{\sim}{\psi}(t)$ is a solution of (4.1) on $[0,b]$. QED

Theorem 1 now follows from Lemmas 4 and 5.

Comment. It should be noticed that the PLCI were shown to converge for some model problems that required some simplifying assumptions on the geometry of the active sites and the extent of the domain—for example, a single active site in an infinite domain. The interval of convergence $[0,b]$ of Theorem 1 agrees precisely with the interval of existence guaranteed by the Miller theory. [11] Thus the PLCI will, according to the theory established here, capture a solution (4.1) for as long as such a solution is guaranteed to exist by Miller's Theory. The extent of the interval of existence depends upon the relationship (4.4c) between the forcing represented by M_o, the reaction represented by M_1, and the diffusion processes embodied in the kernel $\underset{\sim}{g}$

If we were to use the above theory to try to provide estimates for the interval of convergence of the PLCI for practical problems in which the domain is finite, we would find that the estimates are extremely conservative due to the fact that the Dirichlet problem is inherently less stable on an infinite domain than a finite domain [20]. What is probably more important to remember is that the PLCI provide a convergent approximation to the model problems and only break down when existence of a solution is not guaranteed.

D. Numerical Illustration of Convergence

In this section we demonstrate that the PLCI do provide a viable numerical scheme by solving two model problems:

(i) *An initial boundary value problem with a single active site at which a linear reaction occurs.* We consider the scalar initial value problem

$$\begin{aligned} \frac{\partial u}{\partial t} &= D\frac{\partial^2 u}{\partial x^2} + \delta(x-1)Ju \qquad x\varepsilon(0,2) \\ u(x,0) &= \begin{cases} x & 0 \le x \le 1 \\ 1-x & 0 < x \le 2 \end{cases} \\ u(0,t) &= 0 = u(2,t) \end{aligned} \tag{4.8}$$

The analytic solution for this problem can be obtained by exploiting the symmetry of the problem and by using the method of separation of variables:

$$u(x,t) = \sum_{n=1}^{\infty} A_n e^{-\lambda_n^2 Dt} \sin \lambda_n x$$

Here $\{\lambda_n\}_{n=1}^{\infty}$ are solutions to the equation $\tan \lambda_n = 2d\lambda_n/J$ and $A_n = 4(\sin \lambda_n - \lambda_n \cos \lambda_n)/(2\lambda_n^2 - \lambda_n \sin 2\lambda_n)$.
In this example the values $D = 1.0$ and $J = -2.0$ are used.

In Fig. 5 the exact and BE solutions to (4.8) at two different times $t = 0.01$ and $t = 0.1$ are presented. Two different schemes are used to treat the integral in (2.3) that represents the active site:

PWC: the solution is assumed to be constant over the time-step when evaluating the integral in (2.3) that involves R_l.

PWL: a piecewise linear interpolation scheme based on the Caratheodory iteration procedure outlined in (4.3) is used to evaluate the integral in (2.3) that involves R_l.

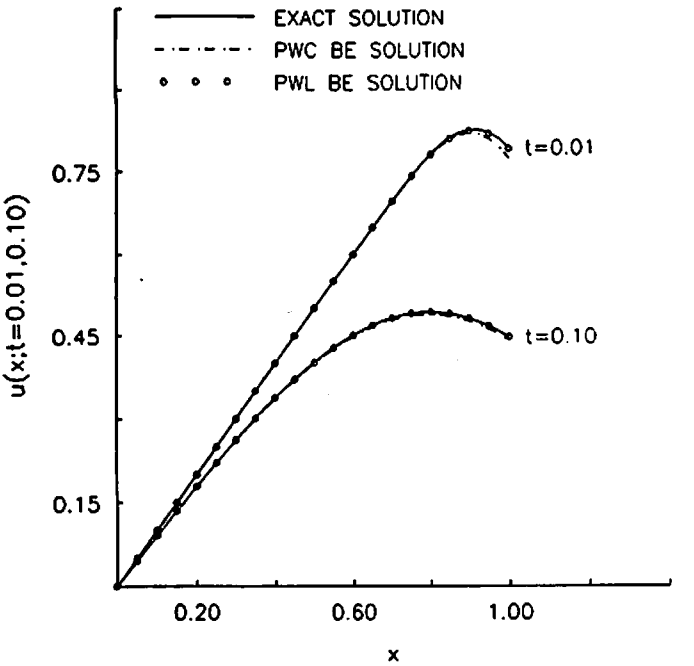

FIG. 5. Exact and PWC and PWL BE solutions at times $t = 0.01$ and $t = 0.1$ for the single linear active site problem (4.8). An accurate BE algorithm based on PWQ integration was used with $a = 1/60$ and $\Delta t = 0.01$ so that $\Theta = 12.0$. The diffusion coefficient used was $D = 1.0$ while $J = -2.0$. After one time-step $t = 0.01$ the maximum error is 2.3% for the PWC BE solution and 0.20% for the PWL BE solution. As time progresses to $t = 0.1$ the error is reduced to 1.3% for the PWC BE solution and 0.06% for the PWL BE solution.

Both of these BE algorithms are explicit in that it is not necessary to solve a system of nonlinear equations at each time-step.

To be able to focus exclusively on the errors introduced by the BE representation of the active site and the explicit PWC and PWL treatment in time of the active site equations, we use an accurate spatial discretization of the BE equations by means piecewise quadratic interpolation. A mesh with $\Delta t = 0.01$ and $a = 1/60$ was used so that $\Theta = 12.0$.

In Fig. 5 we observe that the error committed by the explicit PWC scheme for solving the active site equation is of the order of 2.3% at $t = 0.01$ and is even reduced to 1.3% by $t = 0.1$. The PWL BE solution is virtually indistinguishable from the exact solution in Fig. 5 and has a maximum error at $t = 0.01$ of 0.20% and at $t = 0.10$ of 0.06%. The PWL scheme, based on the piecewise linear Caratheodory iterates analyzed in Section 4, is clearly the better of the two techniques and involves only a marginal increase in computing costs. Naturally the errors observed here can be decreased by decreasing the size of the time-step. If the time-steps required by a particular reaction process are extremely small, then the appropriate domain collocation scheme and mesh must be used. From the theory established in Section 3 small time-steps will require a very fine spatial mesh if piecewise constant or piecewise linear domain cells are used. Extremely fine spatial meshing will not be required if quadratic

cells are used. This simple illustration demonstrates how useful the theory in Section 3 can be when an appropriate meshing strategy is to be determined.

In this problem the constants of (4.4) are $M_0 = 1$ and $M_1 = 4$ so that the interval of convergence guaranteed by the above theory is $[0,\pi/16]$. As was suggested in the remark at the end of Section C this convergence interval is extremely conservative as it assumes an infinite domain, and no account is taken of the sign of J. If $J > 0$ and the domain is infinite, then the solution would become infinite as $t \to \infty$. In contrast, the solution to the problem (4.8) exists [20] for all time, provided $J < (4D/L) = 2$ (where $L = 2$ is the length of the interval). In view of the fact that we established, for the model problem, that the PLCI will capture the solution as long as it exists, we expect in this case that the PLCI will provide a convergent scheme.

(ii) *An initial-boundary value problem with a single active site at which a nonlinear reaction occurs.* We consider the vector initial-boundary value problem

$$\begin{aligned} \frac{\partial u_i}{\partial t} &= D_i \frac{\partial^2 u_i}{\partial u^2} + \delta\left(x - \frac{L}{2}\right) R_i(u_j) \qquad x\varepsilon(0,L) \qquad i,j\varepsilon\{1,2\} \\ u_i(x,0) &= u_i^o(x) \\ u_i(0,t) &= 0 = u_i(L,t) \end{aligned} \tag{4.9}$$

In this problem we choose a reaction term $R_i(u_j)$ associated with the Lotka-Volterra system of nonlinear ordinary differential equations:

$$\begin{aligned} R_1(u_j) &= 4u_1 - 4u_1u_2 \\ R_2(u_j) &= -4u_2 + 4u_1u_2 \end{aligned} \tag{4.10}$$

Although it is not possible to find a closed form solution to (4.9–4.10) it is possible to locate the equilibrium solutions (i.e., those for which $(\partial u_i/\partial t) = 0$; $i = 1,2$). The stability of these equilibria can be investigated by linearizing (4.9) about these equilibrium solutions. We obtain a system of linear partial differential equations that governs the behavior of some small perturbation to the equilibrium solutions. The growth, boundedness, or decay of these small perturbations as $t \to \infty$ determines the stability of the system. It should be remembered that this type of linear stability analysis is inherently local and does not guarantee stability in the large.

We now assume for simplicity that the coupled linearized system can be decoupled into two scalar equations by diagonalization. This will be possible if, for example, $D_1 = D_2$ and the Jacobian

$$J_{ij} = \frac{\partial R_i}{\partial u_j}\Big|_{x=L/2}$$

can be diagonalized by a similarity transformation. Applying the Laplace Transform to the scalar equations we obtain [20] the following sufficient conditions for stability:

$$\text{or} \quad \begin{cases} (1) \quad \dfrac{LJ_i}{2} < D_i \qquad \text{where } J_i \varepsilon \mathbb{R} \\ (2) \quad |\arg(J_i)| > \dfrac{\pi}{4} \quad \text{where } J_i \varepsilon \mathbb{C} \quad \text{and} \quad D_i \neq 0. \end{cases} \tag{4.11}$$

Here J_i are the eigenvalues of the Jacobian.
The two equilibrium solutions of (4.9–4.10) are readily obtained by integrating (2.1) with $\partial u_i/\partial t = 0$:

$$u_i(x) = \begin{cases} A_i x & 0 \leq x \leq L/2 \\ A_i(L - x) & L/2 < x \leq L \end{cases} \tag{4.12}$$

where $(A_1, A_2) = (0, 0)$ or $(A_1, A_2) = 2/L(1 + D_2/L, 1 - D_1/L)$.
In the numerical experiments we choose $D_1 = D_2 = 1.0$, $L = 2$,

$$\text{and} \quad u_i^o(x) = \begin{cases} \psi_i x & 0 \leq x \leq 1 \\ \psi_i(2 - x) & 1 \leq x \leq 2 \end{cases} \qquad \psi_1 = 1.00 \qquad \psi_2 = 1.00$$

For this parameter choice the equilibria are given by (4.12) with $(A_1, A_2) = (0, 0)$ and $(A_1, A_2)(3/2, 1/2)$; and the eigenvalues of the Jacobian are $J_j = (-1)^{j+1}x4$; $J_{1,2} = 2(1 \pm i\sqrt{3})$ respectively. Since the eigenvalues in each case are distinct, the Jacobians in both cases are not defective. Therefore, the stability criteria of (4.11) apply. For the zero solution, stability is not guaranteed by either criterion. In fact, this solution is unstable. However, for the other equilibrium solution, criterion (2) of (4.11) guarantees stability.

Figure 6 presents the phase diagram at the active site of a number of PWL BE solutions in which the time-steps $\Delta t = 0.050$; 0.020; 0.010 and 0.005 are used. We use the same spatial meshing as in example (i) of this section. These solutions correspond to piecewise linear Caratheodory iterates over the time interval $[0, T = 5.0]$ and $J = 100$, 250, 500, and 1000 respectively. All the Caratheodory iterates converge to the stable equilibrium point $(3/2, 1/2)$ predicted by the theory. The convergence (in the sense of Cauchy) of the Caratheodory iterates can be clearly observed in Fig. 6.

As was the case in example (i) of this section, the guaranteed interval of convergence is extremely conservative, namely $[0, (\pi/576)]$. This is due to the infinite domain assumption and the fact that the bound 4.4(b) does not take into account the detailed structure of $R_i(u_j)$. For this finite domain problem the PLCI solution approaches the steady state predicted by the theory outlined above.

V. COMMENTS AND CONCLUSIONS

In this paper we hve performed a convergence analysis of BE schemes for the linear diffusion equation with localized nonlinear reactions. The analysis is divided into two parts:

(i) *The linear diffusion equation.* We use a novel convergence analysis that combines asymptotic methods with Lax's Equivalence Theorem to establish a number of interesting properties of a one-step recursion algorithm appropriate

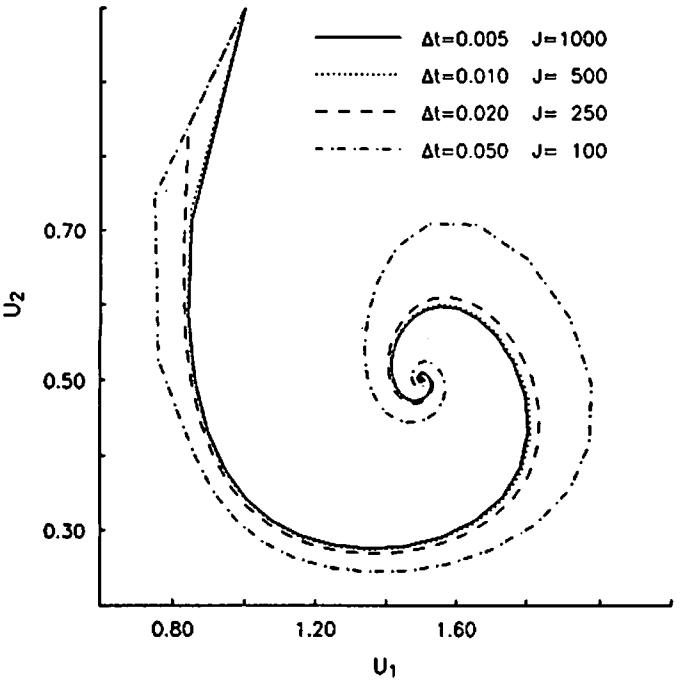

FIG. 6. Phase plots at the active site of PWL BE solutions to (4.9).

$$\text{Here } D_1 = D_2 = 1.0, \quad u_i^o(x) = \begin{cases} \psi_i x & 0 \le x \le 1 \\ \psi_i(2-x) & 1 < x < 2 \end{cases} \quad \psi_1 = 1.0, \quad \psi_2 = 1.0$$

and the Lokta-Volterra reaction term of (4.10) was used. The BE spatial mesh parameters were $a = 1/60$. All the PWL BE solutions approach the stable equilibrium position and the convergence of the PWL Caratheodory iterates can be clearly seen.

for advancing BE solutions when localilzed reactions are present. This analysis provides a theoretical framework for the choice of the appropriate size of time-step. A dimensionless meshing parameter Θ is identified, the magnitude of which governs the performance of the BE scheme.

In particular, PWC and PWL BE schemes are shown to be conditionally convergent having lower asymptotic bounds on the size of time steps. In addition, no restrictions need be placed on how large the time-steps can be, other than for considerations of accuracy. The PWQ BE scheme is shown to be unconditionally convergent, i.e., there is no restriction on the relative sizes of time and spatial meshing. Thus, the payoff for using higher-order spatial interpolation is evident.

The convergence properties of the BE schemes that are predicted by the above convergence theory are verified in numerical experiments. The crucial role of the mesh parameter Θ for PWC and PWL BE schemes is confirmed by these numerical experiments. The phenomenon of numerical diffusion for small values of Θ, which is predicted by the theory for PWC and PWL schemes, can also be observed in the numerical experiments. The amount of excess diffusion

observed numerically and predicted theoretically agrees well for those values of Θ for which the asymptotic expansions used in the theory are still valid. In the numerical experiment the magnitude of the mesh parameter Θ has little effect on the PWQ BE scheme and no excess diffusion is observed. This result is consistent with the theoretical unconditional convergence of the PWQ BE scheme.

The insight gained from this analysis enables us to choose the BE algorithm and meshing strategy best tailored to the needs of a given problem. For example, if we are interested in short-time transient behavior, we should invest in high-order spatial interpolation while the degree of time-interpolation is not as important. On the other hand, if we are interested in achieving a long-time solution rapidly, we should use high order time integration. In this case the degree of spatial interpolation is less important. Finally, if PWC or PWL BE schemes are used, the chosen mesh should satisfy appropriate minimal consistency restrictions on Θ. This analysis therefore enables us to exploit the properties of the one-step recursion schemes for the BE equations that are quite distinct from those of finite differences and finite elements.

(ii) *The diffusion equation with localized nonlinear reactions.* We have analyzed the convergence of an explicit algorithm to advance the solution at localized reaction sites forward in time. To simplify the analysis we assumed a special geometry in which the BE equations were reduced to a nonlinear singular Volterra equation. We established the convergence on a finite time interval of a Caratheodory iteration scheme based on piecewise linear collocation. The length of the interval of convergence is exactly the same as that for which a solution is shown to exist by the theory of Miller [11]. Since the above convergence analysis was performed for a model problem, estimates of the interval of convergence tend to be very conservative if applied directly to practical problems. However, the analysis does establish that the piecewise linear collocation scheme performed well in the approximation of integral equations representing localized nonlinear reactions. A numerical illustration is provided in which the piecewise constant and piecewise linear collocation techniques are applied to a diffusion equation with a localized *linear* reaction. In this case the approximate solutions agree closely with the analytic solution. Piecewise linear Caratheodory iterates are provided for a second problem in which the localized reaction is nonlinear. The convergence of the piecewise linear Caratheodory iterates can be seen clearly in this example. All of the Caratheodory iterates tend to the stable equilibrium position, which can be determined analytically.

The linear convergence analysis developed in this paper provides a useful theoretical framework for choosing the appropriate degree of piecewise polynomial to use in the spatial discretization and meshing strategy for a given problem. Recently the BE algorithm has been demonstrated to be eminently suited to the analysis of realistic linear diffusion equations with localized nonlinear reactions [21]. In the present paper the nonlinear convergence analysis has been performed on a simplified model problem. The analysis provides a theoretical justification for the approximation of BE equations representing localized nonlinear reactions by a scheme using piecewise linear Caratheodory iteration.

APPENDIX A: DISCRETIZATION OF BE EQUATIONS

Let $x_0 < x_1 < \ldots < x_{N-1} < x_N$ be a partition of the interval $[x_0, x_N]$ in which the set of active sites $\{x_{r_l}\}_{l=1}^{L}$ are included as a subset. In accordance with the one time-step recursion algorithm described in Section 3(A), we introduce piecewise polynomial interpolation functions over the rectangular space-time cells $[x_{e-1}, x_e]x[0, \Delta t]$. Within the e^{th} interval $[x_{e-1}, x_e]$ we introduce the nodal points $\{x_e^m\}_{m=1}^{P}$ and over the time interval $[0, \Delta t]$ we introduce the nodal points $\{t^n\}_{n=1}^{Q}$. Here $P - 1$ and $Q - 1$ are the degrees of the spatial and time polynomial approximation respectively. We now define basis functions, X_e^m and T^n:

$$X_e^m\colon X_e^m(x_K^n) = \delta_{eK}\delta_{mn} \qquad T^m\colon T^m(t^n) = \delta_{mn}$$

The resulting interpolants of the functions $u(x,t)$, $(\partial u/\partial x)(x_i,t) = \phi(x_i,t)$ and $f(x,t)$ are obtained:

$$u(x,t_j) = \sum_{e=1}^{N}\sum_{m=1}^{P} X_e^m(x)u(x_e^m,t_j)$$

$$\phi(x_i,t_j+t) = \sum_{n=1}^{Q} T^n(t)\phi(x_i,t_j+t^n) \qquad i = 0,N \tag{A.1}$$

$$f(x,t_j+t) = \sum_{e=1}^{N}\sum_{m=1}^{P}\sum_{n=1}^{Q} X_e^m(x)T^n(t)f(x_e^m,t_j+t^n)$$

Substituting these expressions into (2.3) and assuming homogeneous Dirichlet boundary conditions, we obtain

$$\begin{aligned} u(x,t_{j+1}) = {} & \sum_{e=1}^{N}\sum_{m=1}^{P} G^{em}(x,\Delta t)u^{em}(t_j) + \sum_{i=0,N}\sum_{n=1}^{Q} g_n^i(x)\phi_n^i(t_j) \\ & + \sum_{l=1}^{L}\int_0^{\Delta t} G(x-x_{r_l},\Delta t-\tau)R_l\left(\sum_{n=1}^{Q} T^n(\tau)u(x_{r_l},t_j+t^n)\right)d\tau \\ & + \sum_{e=1}^{N}\sum_{m=1}^{P}\sum_{n=1}^{Q} G_n^{em}(x)f_n^{em} \end{aligned} \tag{A.2}$$

$$\text{Here } G^{em}(x,\Delta t) = \int_{x_{e-1}}^{x_e} G(x-\xi,\Delta t)X_e^m(\xi)\,d\xi$$

$$g_n^i(x) = \int_0^{\Delta t} G(x-x_i,\Delta t-\tau)T^n(\tau)\,d\tau$$

$$\begin{aligned} G_n^{em}(x) &= \int_0^{\Delta t} T^n(\tau)\int_{x_{e-1}}^{x_e} G(x-\xi,\Delta t-\tau)X_e^m(\xi)\,d\xi\,d\tau \\ &= \int_0^{\Delta t} T^n(\tau)G^{em}(x,\Delta t-\tau)\,d\tau \end{aligned}$$

It is possible to evaluate the integrals $G^{em}(x,\Delta t)$ and the self effects $g_n^i(x_i)$ analytically. In the remaining cases the integrands are smooth and can be evaluated using Gauss integration.

Rather than providing the general expressions of G^{em}, etc., we will provide the results in the two special cases $P = Q = 1$ and $P = Q = 2$. These kernels will be used in Section 3 to analyze the convergence of the BEM.

Interpolation by a Constant Function in Space and Time: $P = Q = 1$

In this case

$$x_e^1 = \frac{1}{2}(x_{e-1} + x_e); \qquad X_e^1 = \{H(x - x_{e-1}) - H(x - x_e)\}$$

where H = the Heavyside function.

$$t^1 = \Delta t; \qquad T^1 = \{H(t) - H(t - \Delta t)\}$$

$$(G_{ij})^{e1}(x, \Delta t) = \frac{1}{2}\exp[-\Omega_i \Delta t]\left[\operatorname{erf}\left(\frac{x - x_{e-1}}{2\sqrt{D_i \Delta t}}\right) - \operatorname{erf}\left(\frac{x - x_e}{2\sqrt{D_i \Delta t}}\right)\right]\delta_{ij} \tag{A.3}$$

$$(g_{kl})_1^i(x_i, \Delta t) = \begin{cases} \dfrac{\delta_{kl}}{2\sqrt{D_k \Omega_k}} \operatorname{erf}(\sqrt{\Omega_k \Delta t}) & \Omega_k \neq 0 \\ \left(\dfrac{\Delta t}{\pi D_k}\right)^{1/2} \delta_{kl} & \Omega_k = 0 \end{cases}$$

Interpolation by a Linear Function in Space and Time: $P = Q = 2$

In this case

$$\left.\begin{aligned} x_e^1 = x_{e-1}; \qquad x_e^2 = x_e; \qquad X_e^m &= \frac{\frac{x_e}{2}(1 - \theta_m) - \frac{x_{e-1}}{2}(1 + \theta_m) + \theta_m x}{(x_e - x_{e-1})} \\ t^1 = o; \qquad t^2 = \Delta t; \qquad T^n &= \frac{1}{2}(1 - \theta_n) + \theta_n \frac{t}{\Delta t} \end{aligned}\right\}$$

where

$$\theta_m = \begin{cases} -1 & m = 1 \\ 1 & m = 2 \end{cases}$$

$$\begin{aligned} (G_{kl})^{em}(x, \Delta t) = \frac{1}{2}\exp[-\Omega_k \Delta t]\Bigg\{\Bigg[\operatorname{erf}\left(\frac{x - x_{e-1}}{2\sqrt{D_k \Delta t}}\right) - \operatorname{erf}\left(\frac{x - x_e}{2\sqrt{D_k \Delta t}}\right)\Bigg] X_e^m(x) \\ + \frac{2\theta_m}{(x_e - x_{e-1})}\left(\frac{D_k \Delta t}{\pi}\right) \\ \cdot \left[\exp\left[\frac{-(x - x_{e-1})^2}{4D_k \Delta t}\right] \right. \\ \left. - \exp\left[\frac{-(x - x_e)^2}{4D_k \Delta t}\right]\right]\Bigg\}\delta_{kl} \end{aligned} \tag{A.4}$$

$$(g_{kl})_n^i(x_i, \Delta t) =$$
$$\begin{cases} \delta_{kl}\left\{\dfrac{1}{2\sqrt{D_k\Omega_k}}\operatorname{erf}(\sqrt{\Omega_k\Delta t})\left[\dfrac{1}{2}(1+\theta_n) - \dfrac{\theta_n}{2\Omega_k\Delta t}\right] + \dfrac{\theta_n \exp[-\Omega_k\Delta t]}{2\Omega_k\sqrt{\pi D_k\Delta t}}\right\}, \\ \Omega_k \neq 0 \\ \delta_{kl}\dfrac{1}{2}\left(1+\dfrac{\theta_n}{3}\right)\left(\dfrac{\Delta t}{\pi D_k}\right)^{1/2}, \qquad \Omega_k = 0 \end{cases}$$

APPENDIX B: INFLUENCE MATRICES OF PIECEWISE POLYNOMIAL COLLOCATION METHOD

Consider a uniform spatial mesh $x_n = n \cdot 2a$, $n \in \mathbb{Z}$ and a time-step Δt. We define the following dimensionless mesh parameter Θ as follows

$$\Theta := \frac{2\sqrt{D\Delta t}}{a}$$

and introduce the notation

$$I_m^n := \frac{1}{\sqrt{\pi}}\int_{m/\Theta}^{n/\Theta} \exp(-s^2)\,ds$$

Exploiting the convolution property $G_{mn} = G(|m-n|)$ of the influence matrices, we can write them as follows:

(1) Piecewise constant basis functions:

$$G(n) = I_{2n-1}^{2n+1}$$

(2) Piecewise linear basis functions:

$$G(n) = (n+1)I_{2n}^{2n+1} - (n-1)I_{2(n-1)}^{2n} + \frac{\Theta}{4\sqrt{\pi}}$$
$$\left\{\exp\left[-\frac{4(n+1)^2}{\Theta^2}\right] - 2\exp\left[-\frac{4n^2}{\Theta^2}\right] + \exp\left[-\frac{4(n-1)^2}{\Theta^4}\right]\right\}$$

(3) Piecewise quadratic basis functions*:

$$G(2n+1) = \left\{n(2n-1) + \frac{\Theta^2}{4}\right\}I_{2n-1}^{2n+1} + \left\{(n+1)(2n+3) + \frac{\Theta^2}{4}\right\}I_{2n+1}^{2n+3}$$
$$+ \frac{\Theta}{2\sqrt{\pi}}\left\{-3\exp\left[-\frac{(2n+1)^2}{\Theta^2}\right] + (n+1)\exp\left[-\frac{(2n+3)^2}{\Theta^2}\right]\right.$$

*Note that the influence matrices G with odd arguments represent the effect of basis functions located at the endpoints of the cells evaluated at midpoints of cells, while those with even arguments give the effect of basis functions located at cell midpoints evaluated at cell midpoints.

$$- n \exp\left[-\frac{(2n-1)^2}{\Theta^2}\right]\Bigg\}$$

$$G(2n) = -\left(4n^2 - 1 + \frac{\Theta^2}{2}\right) I_{2n-1}^{2n+1} + \frac{\Theta}{2\sqrt{\pi}}$$

$$\left\{-(2n-1)\exp\left[-\frac{(2n+1)^2}{\Theta^2}\right]\right.$$

$$\left. + (2n+1)\exp\left[-\frac{(2n-1)^2}{\Theta^2}\right]\right\}$$

The authors acknowledge support for this research from the Department of Energy. The first author also gratefully acknowledges the support of the CSIR of South Africa, the Fulbright Foundation, and the NSERC of Canada.

References

[1] P. Ortoleva and J. Ross, "Local structures in chemical reactions with heterogeneous catalysis," *J. Chem. Phys.*, **56**, 4397 (1972); "Phase waves in oscillatory chemical reactions," **58**, 5673 (1973).

[2] K. Bimpong-Bota, P. Ortoleva, and J. Ross, "Far-from-equilibrium phenomena at local sites of reaction," *J. Chem. Phys.*, **60**, 3124 (1974).

[3] K. Bimpong-Bota, A. Nitzan, P. Ortoleva, and J. Ross, "Cooperative phenomena in arrays of catalytic sites," *J. Chem. Phys.*, **66**, 3650 (1977).

[4] P. K. Banerjee and R. Butterfield, *Boundary Element Methods in Engineering Science*, (McGraw Hill, U.K., 1981).

[5] C. A. Brebbia and S. Walker, *Boundary Element Methods in Engineering*, Newnes-Butterworth, London, 1980.

[6] H. L. G. Pina and J. L. M. Fernandes, "Applications in transient heat conduction," in C. A. Brebbia, Ed., *Topics in Boundary Element Research*, Vol. 1, Springer-Verlag, Berlin, 1984.

[7] C. A. Brebbia and L. C. Wrobel, "Steady and unsteady potential problems using the boundary element method," in C. Taylor, *Recent Advances in Numerical Methods in Fluids*, Swansea, 1979.

[8] P. D. Lax and R. D. Richtmyer, *Communications on Pure and Applied Mathematics*, IX, 267, 1956; L. Lapidus and G. F. Pinder, *Numerical Solution of Partial Differential Equations in Science and Engineering*, Wiley Interscience, New York (1982).

[9] D. N. Arnold and P. J. Noon, *Coecivity of the single layer heat potential*, Report MD87-45-DNA/PJN TR87-45, Department of Mathematics, University of Maryland, College Park, 1987.

[10] M. Costabel, K. Onishi, and W. L. Wendland, "A boundary element collocation method for the Neumann problem of the heat equation," preprint.

[11] R. K. Miller, *Nonlinear Volterra Integral Equations*, W. A. Benjamin, Menlo Park, California, 1971.

[12] F. John, *Partial Differential Equations*, 4th ed., Springer-Verlag, New York, 1985.

[13] W. E. Williams, *Partial Differential Equations*, Oxford University Press, 1980.

[14] C. T. H. Baker, *The Numerical Treatment of Integral Equations*, Oxford University Press, 1977.

[15] M. A. Golberg, "A survey of numerical methods for integral equations," in M. A. Golberg, Ed., *Solution Methods for Integral Equations*, Plenum, 1979.

[16] R. Vichnevetsky and J. B. Bowles, *Fourier Analysis of Numerical Approximations of Hyperbolic Equations*, Siam, Philadelphia, 1982.

[17] C. M. Bender and S. A. Orszag, *Advanced Mathematical Methods for Scientists and Engineers*, McGraw-Hill, NY, 1978.

[18] G. D. Smith, *Numerical Solution of Partial Differential Equations: Finite Difference Methods*, 2nd ed., Oxford University Press, 1978.

[19] E. Kreysig, *Introductory Functional Analysis with Applications*, John Wiley & Sons, NY, 1978.

[20] A. Peirce and H. Rabitz, "Effect of defect structures on chemically active surfaces: A continuum approach," *Phys. Rev. B*, **38**, 1734 (1988).

[21] A. P. Peirce and H. Rabitz, "An analysis of the effect of defect structures on catalytic surfaces by the boundary element technique," *Surface Science*, **202**, 1-31 (1988); "Modeling the effect of changes in defect geometry on chemically active surfaces by the boundary element technique," **202**, 32-57 (1988).